A Thesis for the Degree of Master of Science

Structural and retrogradation properties of sonicated high-amylose corn starch with temperature-cycling treatment

초음파 처리 고아밀로스 옥수수 전분의 온도 사이클링 처리에 의한 구조적 특성과 노화 특성

February, 2017

Han, Kyu Tae

Department of Agricultural Biotechnology

Seoul National University

농학석사학위논문

Structural and retrogradation properties of sonicated high-amylose corn starch with temperature-cycling treatment

초음파 처리 고아밀로스 옥수수 전분의 온도 사이클링 처리에 의한 구조적 특성과 노화 특성

지도교수 문 태 화
이 논문을 석사학위 논문으로 제출함

2017년 2월
서울대학교 대학원
농생명공학부
한 규 태

한 규 태의 석사학위 논문을 인준함
2017년 2월

위 원 장 최 상 호 인

부위원장 문 태 화 인

위 원 장 판 식 인

A Thesis for the Degree of Master of Science

Structural and retrogradation properties of sonicated high-amylose corn starch with temperature-cycling treatment

by

Han, Kyu Tae

Advisor: Tae Wha Moon, Professor

Submitted in Partial Fulfillment of the Requirement
for the Degree of Master of Science

February, 2017

Department of Agricultural Biotechnology

Seoul National University

ABSTRACT

In this study, high-amylose corn starch (HACS) was sonicated, and then retrograded by isothermal storage and temperature-cycling for 16 days. After the sonication, the retention time of both amylopectin (AP) and amylose (AM) peak increased in gel permeation chromatography because of the reduced molecular weight of starch. Percentages of α-1,4 glycosidic bonds in ^{1}H NMR spectroscopy decreased slightly as the sonication time increased. Breakdown of AM double helices provided more space to form iodine-starch complexes, resulting in a higher apparent amylose content in sonicated starch. Crystallites of AP collapsed gradually, and those of AM disappeared in differential scanning calorimetry after the sonication. Though HACS samples maintained B-type polymorph, decreases in major peak intensities and relative crystallinity were observed by X-ray diffractometry during sonication. ^{13}C CP/MAS NMR spectroscopic analysis revealed that the proportion of double helical structure also reduced with the extended sonication time. A gradual decrease in average DP determined by high-performance anion-exchange chromatography could be caused by the vulnerability of outer branched chains to sonication. S6, which was sonicated for 60 min, and then retrograded with native HACS, showed the most significant difference in structural properties.

Nucleation was accelerated by the numerous AM nuclei formed by disruption of most AM double helices during sonication. Hydrolysis of α-1,4 linkage in amorphous region reduced the length of AM random coil, which was transformed to AM single helix fast and made AM double helices by combining with other single helices broken by sonication. Also, disintegration of cluster structure in AP by hydrolysis of amorphous region led to dense arrangement of AP in propagation step. Thus, transition enthalpy, major peak intensities, relative crystallinity, proportion of double helical structure, and RS contents were elevated during the retrogradation of S6. Moreover, compared with isothermal storage, both nucleation and propagation were promoted by temperature-cycling, and consequently resulted in a higher extent of retrogradation. Higher nucleation and propagation rates were also shown in sonicated and temperature-cycling treated groups using an irreversible consecutive reaction model, supplementing the Avrami kinetics model. S6-TC16 which was subjected to both sonication and temperature-cycling for 16 days, therefore, revealed the most striking retrogradation characteristics.

Sonication treatment induced the proper structural changes for the retrogradation. Structural and retrogradation characteristics and RS contents also changed to a great extent in temperature-cycling compared with isothermal storage. This study provided the basic understanding regarding

the retrogradation of sonicated starch and a kinetic model for temperature-cycled retrogradation. Moreover, RS content obtained suggests a new practical application of sonicated starch.

Keywords: sonication, high-amylose corn starch, temperature-cycling retrogradation, Avrami kinetics model, irreversible consecutive reaction model, structural properties, resistant starch

Student Number: 2015-21802

CONTENTS

LIST OF FUGURES

LIST OF TABLES

INTRODUCTION

Starch is an important reserve polysaccharide of higher plants and is, after cellulose, the second most abundant carbohydrate in the biosphere. As a widely available agricultural commodity and an excellent energy source for human diet, it consists of two α-glucans, amylose (AM) and amylopectin (AP). AM is the linear chain of consecutive α-1,4 glycosidic bonds, and forms single double helices. On the other hand, AP has branched chain structure of α-1,6 linkages and linear α-1,4 chain. Starch is produced by plants in a granular form, and starch granule is composed of alternating amorphous region and crystalline region where molecules are tightly bonded together (Manners, 1989).

Ultrasound is a mechanical wave with a frequency above 16 kHz providing beneficial influences to food processing and preservation by modifying the composition and structure of products. As an emerging technology, it could be used in many food processing operations including emulsification, freezing, and drying (Chemat et al., 2011). In industrial scale, vibration of ultrasound is applied to defoaming of food product by burst of bubble, and clear cutting or slicing of sticky foods, which have high adherence to knife (Arnold et al., 2009; Riera et al., 2006; Schneider et al., 2008). Also, permeability of membrane filtration is assisted by sonication in extraction of

apple pulp, and whey solution (Kyllönen et al., 2005; Muthukumaran et al., 2005). Furthermore, inactivation of pathogenic bacteria in food is achieved by sterilization and pasteurization process with sonication, in related to food preservation (Mañas et al., 2000). Sonication treatment does not release any chemical byproduct, and is estimated as environment-friendly technology (Bartsch & Schmidt-Naake, 2006).

Sonication treatment, different from other physical modifications, is accompanied with chemical depolymerization in starch suspension (Zheng et al., 2013). Firstly, physical degradation caused by bubble cavitation destroys the starch structure. Cavitation, i.e., the collapse of microbubbles, partially destroys the physical structure, and numerous fissures, cracks, pores, or depressions are observed on the starch surface after sonication (Sujka & Jamroz, 2013). Shear force caused by the burst of the microbubbles breaks down the covalent bonds in polymeric materials. Cavitation effect depends on sonication condition of frequency, power, amplitude, and time (Hu et al., 2013). Secondly, chemical degradation also was caused by the chemical reaction between starch and radicals (•OH, •O, •HO_2) generated from the bubble cavitation. Radicals penetrate into the path formed by physical depolymerization, and react with covalent bonds between starch molecules. It results in the reduction of viscosity and molecular weight, increment of water permeability, fat absorbability, swelling power, and solubility (Isono et

al., 1994; Peres et al., 2015; Sujka & Jamroz, 2013). Though these characteristics were ascertained by many studies, additional properties have not been observed in recent years. Moreover, necessities for better exploration the effect of sonication on starch in several aspects are on the rise (Zhu, 2015). Influence of sonication on cluster structure of AP, susceptibility of AM to sonication, and alteration of V-type AM inclusion complex with endogenous lipids under sonication are needed to be investigated. Furthermore, radical generated by sonication could depolymerize starch chains and how sonication affects the branched chain length distribution is required.

On the other hand, a decrease in molecular weight accelerates the retrogradation (Chang & Lin, 2007; Kitamura et al., 1994; Zhang & Jackson, 1992). Thus, it is hypothesized that reduced molecular weight owing to the sonication treatment could increase the degree of retrogradation. Zhu (2015) emphasized that how the molecular changes of starch chains incurred by sonication led to altered retrogradation of starch was not studied, and better understanding of the molecular basis of the changes in retrogradation affected by sonication is needed.

There are several methods to alter the characteristics of starch including physical, chemical and enzymatic modification. Physical modification, such as heat-moisture treatment, annealing and pregelatinization, provides

structural changes without the covalent linkages (Eliasson & Gudmundsson, 2006). Also, alteration of hydrogen bonding induced by physical modification could not show its capability in gelatinization, which is the heating process breaks the hydrogen bonding before retrogradation. In chemical degradation of starch, both α-1,4 bonds and α-1,6 bonds are susceptible to chemical treatment (Kulp & Ponte, 2000). α-1,6 linkages are the inherence of AP, and debranching of these bonds makes the characteristics of AP absent. In addition, there are inevitable side reactions of complex or cross-liking between starch and chemical reagents (Zhang et al., 2012). Enzymatic and chemical degradation caused a very broad distribution of molecular weights (Ba et al., 2013; Nitsch, 1995), and undesired low molecular components have to be removed by organic solvents (acetone, ethanol) because these fractions inhibit the retrogradation (Xu et al., 2012; Yao et al., 2003). In addition, elimination of low molecular fraction results in the loss of the starch and the purification have to be performed for the removal of solvents. Compared to chemical and enzymatic degradation, sonication treatment does not require the addition of reagents as a green technology, and therefore avoids purification process of the degraded samples. No side reaction takes place, and sonication present the advantage to be very simple owing to the dispersion or deagglomeration of suspension during sonication (Poinot et al., 2013).

Retrogradation is an unavoidable phenomenon during cooling and storage of the cooked starch or starchy foods. Starch chains in the gelatinized paste reassociate and form more ordered structure during retrogradation. It is influenced by inherent starch properties such as starch crystallinity, ratio of AP to AP, and botanical origin (Fredriksson et al., 1998; Inaba et al., 1994). Also, starch concentration, presence of other food ingredients, storage conditions including temperature, time, and water content affect the degree of retrogradation (Chang & Liu, 1991; Silverio et al., 2000; Zhou et al., 2011). Sensory property of food is modified by retrogradation, and it consequently could be applied in food such as breakfast cereals and parboiled rice (Karim et al., 2000).

AM and AP play different roles in retrogradation. In short-term retrogradation, nucleation occurs in the first 2 days. AM irreversibly and rapidly reassociates to form crystal nuclei, and thus food texture is changed promptly in this step (Fearn & Russell, 1982). Nucleation is known as the rate-determining-step of retrogradation (Miles et al., 1985). Long-term retrogradation including propagation and maturation is observed following nucleation. Crystalline region of AP grows slowly around the AM crystal nucleus and forms a perfect crystallite. To be specific, outer chains of AP molecules interact with amylose nucleus to form a network, and it is referred to co-crystallization. Rheological and structural changes are revealed in this

step (Fan & Marks, 1998). The overall crystallization rate of starch mainly depends on the nucleation and propagation rate (Eerlingen et al., 1993). Nucleation and propagation are favored at the temperature near glass transition temperature (T_g), and melting temperature (T_m), respectively (Baik et al., 1997; Durrani & Donald, 1995; Silverio et al., 2000). Therefore, stepwise nucleation and propagation could be obtained by temperature-cycled (TC) retrogradation between T_g and T_m, which would accelerate the rate of retrogradation (Zhou et al., 2010). Also, gradual growth of crystalline regions by TC retrogradation results in the formation of perfect starch crystallites. High-amylose corn starch (HYLON V) has strong tendency to retrograde owing to the more than 50% AM content, and its almost equal ratio of AM and AP is suitable for the investigation of TC retrogradation. Though Avrami kinetics model has been used to the calculation for the rate of overall retrogradation in many previous studies, this model could not analyze the rates of nucleation and propagation step of TC retrogradation (Zhang et al., 2015; Zhang & Jackson, 1992). Thus, irreversible consecutive reaction model of chemical reaction engineering was applied to this current study to estimate the rates of both step of TC retrogradation.

Starch regains an ordered structure, that is more resistant to enzymatic digestion during retrogradation (Park et al., 2009). It is called resistant starch (RS), which is a portion of starch that cannot be digested by amylases and

absorbed in the upper digestive tract, small intestine (Englyst et al., 1982). It passes and reaches the colon and is fermented to short-chain fatty acids by microbiota (Xie et al., 2014). RS gives many health benefits to human including improving of the insulin sensitivity and reducing the cardiovascular diseases (Granfeldt et al., 1995; Hasjim et al., 2010; Johnston et al., 2010; Nugent, 2005; Sharma et al., 2008; Skrabanja et al., 2001). Butyrate produced in the large intestine provides the energy for colonocytes, which is protective against colorectal cancer (Brouns et al., 2002). RS helps body fat consumption, and decreases the postprandial blood glucose, insulin elevation, and body weight (Fuentes-Zaragoza et al., 2011; Maki et al., 2012). Also, it prevents type 2 diabetes, improves abnormal glucose tolerance, and manages the obesity (Higgins, 2004; Kim et al., 2003). The daily intake of RS by Americans is 5 g per day, which is much less than the minimum of 6 g of RS per meal recommended for health benefits (Murphy et al., 2008).

RS is classified into five subcategories, called RS1, RS2, RS3, RS4, and RS5: RS with a starch structure covered with a hull, such as in whole-grain flour and unpolished rice, is classified as RS1; starch with a high crystallinity and amylose content is RS2; retrograded starch produced by cooling gelatinized starch is referred to RS3; chemically modified starch is RS4; and complexation of amylose and lipid is RS5 (Birt et al., 2013; Brown et al., 1995; Englyst et al., 1992). The present study focuses on RS3, which is the

most enzyme-resistant starch fraction (Sajilata et al., 2006) formed by retrogradation of native and sonicated starches through isothermal storage and temperature-cycling condition.

The objectives of current study were to investigate the effect of sonication treatment on the structural properties of high-amylose corn starch (HACS) and to assess the influences of temperature-cycling on the retrogradation behaviors and resistant starch content of sonicated HACS. This study would contribute to understanding the structural alteration of starch induced by sonication treatment. Overall retrogradation process including nucleation and propagation during TC retrogradation is also comprehended by irreversible consecutive reaction model. Dual modification of sonication and retrogradation provides RS as a new application of sonicated starch.

MATERIALS AND METHODS

1. Materials

HYLON V was obtained from Ingredion (Westchester, IL, USA), and resistant starch assay kit was purchased from Megazyme (Wicklow, Ireland).

2. Methods

2.1. Preparation of sonicated starch

A 20 kHz sonicator VCX-400 (Sonics & Materials, Inc., Newtown, CT, USA) coupled with a probe (tip diameter of 13mm) was used in the sonication of 10% HACS (w/w) suspension. Energy input was 400W, and amplitudes were 70%. Starch suspensions were sonicated for 10-60 min at 10 min interval and named S1, S2, S3, S4, S5, and S6. Each sample after sonication process was washed three times with distilled water, lyophilized, ground, and passed through a 100-mesh sieve.

2.2. Preparation of starch samples by isothermal storage and temperature-cycled retrogradation

Starch suspension (20%, w/w) was fully gelatinized by heating in boiling water for 30 min followed by autoclaving at 121°C for 30 min. The

gelatinized starch was cooled to room temperature, hermetically sealed, and stored under different temperature conditions: constant temperature of 4°C or cycles of 4°C for 2 days and subsequent 70°C for 2 days. The samples were named according to the storage conditions and retrogradation days of native starch (N) (N-0, N-I4, N-I8, N-I12, N-I16, N-TC4, N-TC8, N-TC12, N-TC16) and S6 (S6-0, S6-I4, S6-I8, S6-I12, S6-I16, S6-TC4, S6-TC8, S6-TC12, S6-TC16). Each sample after retrogradation process was lyophilized, ground and passed through a 100-mesh sieve.

2.3. Determination of molecular weight distribution

Molecular weight distribution chromatograms of starch were obtained by using the Thermo Dionex HPLC Ultimate 3000 Refractive index (RI) system (Dionex, Sunnyvale, CA, USA) with serially connected Waters Ultrahydrogel 1000, 500, 120 gel-permeation chromatography (GPC) column (7.8x300 mm, Waters, Milford, MA, USA). Starch (0.05 g) was suspended in 4.5 mL of 95% dimethyl sulfoxide (DMSO). The suspension was mechanically stirred while heating in a boiling water bath for 1 h and then stirred on a magnetic stirrer for 24 h at 25°C to prepare a starch solution. An aliquot (2 mL) of the starch solution was mixed with absolute ethanol (8 mL) to precipitate the starch, and then centrifuged (14,000 xg, 10 min). The precipitated starch was dissolved in distilled water (10 mL) and stirred on a

magnetic stirrer for 30 min, and the solution was filtered through a 5.0 μm nylon membrane syringe filter (Sigma–Aldrich Chemical Co., St. Louis, MO, USA) to remove the insoluble residues. The supernatant (20 μL) was then injected into the column at 40°C. Sodium azide solution (0.1 M) was used as an eluent at a flow rate of 1 mL/min.

2.4. Proton nuclear magnetic resonance (^{1}H NMR) spectra

Proton nuclear magnetic resonance (^{1}H NMR) spectra were obtained using an AVANCE 600 spectrometer (Bruker, Rheinstten, Germany) operating at 600 MHz following the method of Gidley (1985) with slight modification. For sample pretreatment, 5 mg of sample was fully gelatinized in 1 mL of deuterium oxide (D_2O) by heating in boiling water for 30 min and autoclaving at 121°C for 30 min. Starch suspension was centrifuged (3,000 xg, 10 min), and then supernatant (0.5 mL) was analyzed. Panose (TCI, Tokyo, Japan) was used as standard.

2.5. Determination of apparent amylose content

Apparent amylose contents were measured according to the colorimetric method outlined by AACC Approved Method 61-03 (AACC, 2000). Starch (20 mg) was dispersed in absolute ethanol (0.2 mL), and then 1 M NaOH

(1.8 mL) was added to the mixture, and was heated in boiling water for 10 min with intermittent vortexing. After boiling, the dispersion was cooled to room temperature for 30 min. The cooled starch dispersion (1 mL) was diluted to 10 mL with distilled water. An aliquot (0.5 mL) of the diluted starch solution was combined with 1 M acetic acid (0.1 mL) and diluted again to 10 mL with distilled water. Lugol's solution (0.2 mL; 0.2% I_2 + 2.0% KI) was added and held for 20 min in the dark. The absorbance of the color-developed starch solution was measured at 620 nm. The apparent AM content of the starch sample was determined from a standard curve prepared with amylose from potato and amylopectin from maize (Sigma–Aldrich Chemical Co., St. Louis, MO, USA).

2.6. Evaluation of thermal transition properties

Thermal transition properties of samples were examined using a differential scanning calorimeter (DSC, Diamond DSC, Perkin-Elmer, Waltham, MA, USA). Each sample (10 mg) was weighed in a stainless steel pan (03190029, Perkin-Elmer), and 30 μL of distilled water was added. The sample pan was sealed and kept at room temperature overnight for moisture equilibrium. An empty stainless steel pan was used as a reference, and indium was used for calibration. Samples were heated from 20°C to 180°C at 10°C/min. After the first heating, sonicated starches were additionally cooled from 180°C to -

30°C at a rate of 20°C/min and rescanned from -30°C to 40°C at 10°C/min. The onset temperature (T_o), the peak temperature (T_p), the conclusion temperature (T_c), and the melting enthalpy (ΔH) were recorded from the first scan. The glass transition temperature (T_g) was taken from the second scan of a sonicated sample by measuring the midpoint of baseline shift. Enthalpy of retrogradation samples was used to plot the following two models; Avrami kinetics model and irreversible consecutive reaction model.

The Avrami equation of polymer crystallization was used to study starch retrogradation kinetics. Equation can be written as follows (Jankowski & Rha, 1986):

$$\frac{\Delta H_t}{\Delta H_\infty} = 1 - e^{-kt^n}$$

where t is time (day), k is rate constant (day^{-1}), n is Avrami exponent, ΔH_t is enthalpy at time t (J/g), and ΔH_∞ is limiting enthalpy (J/g).

When the rate equations for the three components (gelatinized starch, amylose nuclei, and retrograded starch) of retrogradation, as an irreversible consecutive reaction, are written and the differential equation obtained is solved by the stoichiometric relations between the concentrations of reacting components, the following equation is obtained using the solution of differential equation presented by (Levenspiel, 1999):

$$\frac{\Delta H_t}{\Delta H_g} = 1 + \frac{k_2}{k_1 - k_2} e^{-k_1 t} + \frac{k_1}{k_2 - k_1} e^{-k_2 t} \quad \cdots\cdots\cdots\cdots (1)$$

where k_1 is nucleation rate constant (day^{-1}), k_2 is propagation rate constant (day^{-1}), ΔH_t is enthalpy at time t (J/g), and ΔH_g is gelatinization enthalpy (J/g).

Limiting enthalpy (ΔH_∞) of native and S6 sample for the analysis of two models was obtained by 60 days retrogradation of each sample (N-∞, S6-∞). Non-linear curve fitting was performed by using SigmaPlot 12.5 software (Systat Software Inc., San Jose, CA, USA). Plotting was conducted by assorting samples into 4 groups of N-I group (N-I4, N-I8, N-I12, N-I16), N-TC group (N-TC4, N-TC8, N-TC12, N-TC16), S6-I group (S6-I4, S6-I8, S6-I12, S6-I16) and S6-TC group (S6-TC4, S6-TC8, S6-TC12, S6-TC16). N-0 and N-∞ were applied to curve fitting of N-I and N-TC groups. Also, S6-0 and S6- were used to plotting of S6-I and S6-TC groups.

2.7. X-ray diffraction patterns and relative crystallinity

X-ray diffraction analysis was conducted using a powder X-ray diffractometer (New D8 Advance, Bruker, Karlsruhe, Germany) at 40 kV and 40 mA. The sample was scanned through 2θ range from 3° to 33° with a 0.02° step size and a count time of 2 sec. The area was calculated using the software developed by the instrument manufacturer (EVA, 2.0). The relative

crystallinity was calculated according to the following equation (Nara & Komiya, 1983).

$$\text{Relative crystallinity (\%)} = \frac{A_c}{A_a + A_c} \times 100$$

A_a: area of amorphous region A_c: area of crystalline region

Major peak intensities were calculated from the ratio of diffraction peak area to total diffraction peak area, namely crystallinity (%) of the major peak (Cheetham & Tao, 1998; Jiranuntakul et al., 2011). It was calculated using the ProFit software (Koninklijke Philips N.V., Amsterdam, Netherlands)

2.8. Solid-state ^{13}C cross-polarization and magic-angle spinning (CP/MAS) nuclear magnetic resonance (NMR) spectra

A Bruker AVANCE 400 WB (Bruker, Karlsruhe, Germany) equipped with CP-MAS accessories was used for ^{13}C CP/MAS NMR analysis. Cross-polarization (CP), magic angle sample spinning (MAS), and high power decoupling conditions were used to observe NMR spectra (single scan). The acquisition time was 35 ms, time domain points 2.2 k, and line broadening 10 Hz. The samples were spun at a rate of 5 kHz at room temperature in a 4-mm rotor with a spectral width of 3.1 kHz. The ordered (double-helical) to amorphous ratio was obtained by comparison between spectra of sample and amorphous starches (Gidley, 1985; Gidley & Bociek, 1985). The data were

processed and calculated of integrated peak areas using the processing tools included in the Topspin 1.3 software (Bruker, Karlsruhe, Germany).

2.9. Determination of branched chain length distribution

The branched chain distribution of the starch samples was determined after debranching by isoamylase using a high-performance anion exchange chromatography system (Dionex-300, Dionex, Sunnyvale, CA, USA) with a pulsed amperometric detector. Starch samples (15 mg) were dissolved in 90% dimethyl sulfoxide (3 mL) and boiled for 30 min. Ethanol (15 mL) was added to the solution and centrifuged at 10,000 ×g for 10 min. The starch pellet was resuspended with distilled water (1.5 mL) and 50 mM sodium acetate buffer (1.5 mL, pH 4.3) and boiled for 15 min mixed. Isoamylase (30 μL) was added to the starch suspension and then incubated at 45°C and 30 rpm for 2 h in a water bath. The enzyme reaction was stopped by boiling for 10 min. The debranched sample was filtered through a 0.45-μm membrane filter and analyzed using high performance anion exchange chromatography with pulsed amperometric detection on a Carbo-Pack PA1 anion-exchange column (4×250 mm, Dionex, Sunnyvale, CA, USA) with a pulsed amperometric detector. This analysis was performed by using a gradient increase of 600 mM sodium acetate in 150 mM NaOH solution against 150 mM NaOH for sample elution as follows: 0-20% for 0-5 min, 20-45% for 5-

30 min, 45-55% for 30-60 min, 55-60% for 60-80 min, 60-65% for 80-90 min, 65-80% for 90-95 min, and 80-100% for 95-100 min. The values of DP were designated using a mixture of maltooligosaccharides (DP 1-7, Sigma Chemical) as standard. PeakNet software (version 5.11, Dionex, Sunnyvale, CA, USA) was used for calculation of peak areas. Number-based average DP (DP_n) was determined by following equation.

$$DP_n = (\%A_i \times DP_i) / 100$$

A_i : peak area / total area (i: 1, 2, 3 …)

2.10. Assay of resistant starch (RS) content

An RS assay kit following the AOAC Method 2002.02 (McCleary et al., 2002) and AACC Method 32-40.01 (AACC, 2002) was used to measure RS content. Sample (100 mg) was incubated with 4 mL pancreatic α-amylase (10 mg/mL) containing amyloglucosidase (AMG, 3 U/mL) at 37°C for 16 h with constant shaking. The reaction was stopped with 4.0 mL of ethanol (99%, v/v) and centrifuged (1,500 xg, 10 min). Then, the sample was washed twice with ethanol (50%, v/v), and centrifuged (1,500 xg, 10 min). The separated pellet was further dissolved with 2 M KOH (2 mL) for 20 min. Dissolved pellet was mixed with 1.2 M sodium acetate and hydrolyzed to glucose by 0.1 mL AMG (3,300 U/mL) at 50°C for 30 min. The hydrolyzates were diluted to 100 mL and centrifuged (1,500 xg, 10 min), and the released

glucose was analyzed using a glucose oxidase-peroxidase (GOPOD) reagent kit.

2.11. Statistical analysis

All experimental data were analyzed by analysis of variance (ANOVA) and expressed as mean ± standard deviation of replicate measurements. The data of retrograded samples were analyzed using a 3-way (presence of sonication, retrogradation period, and storage type) multivariate analysis of variance (MANOVA) applied with interaction of 2 factors. Significant differences among mean values were compared using Tukey`s honest significant difference (HSD) test ($p<0.05$). Principal component analysis (PCA) was performed on the experimental data to summarize the relationship between the sample and its structural and retrogradation properties. All statistical analyses were conducted by IBM SPSS statistics version 22.0 (IBM, Manhattan, NY, USA).

RESULTS AND DISCUSSION

[Section I] Structural properties of sonicated high-amylose corn starch

1. Molecular weight distribution

For characterization of the molecular weight distribution of native and sonicated starch samples, the changes in their gel permeation chromatograms (GPC) are presented in Figure 1, and the retention time of each peak is shown in Table 1.

Because of its large molecular weight, AP was eluted at the first peak (peak I), and the second peak (peak II) was considered to be AM (Bradbury & Bello, 1993; Czuchajowska et al., 1998; Leong et al., 2007; Lin & Czuchajowska, 1997; Mali et al., 2004). Retention time of peak I for sonicated starches was 0.34 - 0.50 min longer as compared with native starch (Isono et al., 1994; Peres et al., 2015). Also, peak II displayed 0.34 - 0.46 min longer retention time than that for native starch did.

An increase in retention time of each peak indicated that the molecular weight was reduced by sonication. Depolymerization of starch in suspension was presumably caused by mechanical degradation by microbubble

cavitation. Collapse of microbubble makes cavitation effects, which are fissures, pores, and depressions on the starch surface due to the partial physical destruction, because shear forces by the burst of the microbubbles also break covalent linkage between glucose molecules in starch (Luo et al., 2008). In addition, radicals (•OH, •O, •HO_2) generated by the microbubble cavitation react with starch, causing chemical degradation. The radicals penetrate into the path formed by bubble cavitation and degrade the glycosidic bonds located inside of starch, and this phenomenon plays a major role in reduction of molecular weight of starch (Czechowska-Biskup et al., 2005; Kardos & Luche, 2001).

Retention time of two peaks was extended due to the longer sonication time, but the increases in retention time were 0.06 min for AP and 0.08 min for AM. Intermediate materials (IM), which were not clearly separated from peaks of AM and AP, were detected as an elevated baseline or a small hump between peak I and peak II suggesting an increase in retention time by sonication.

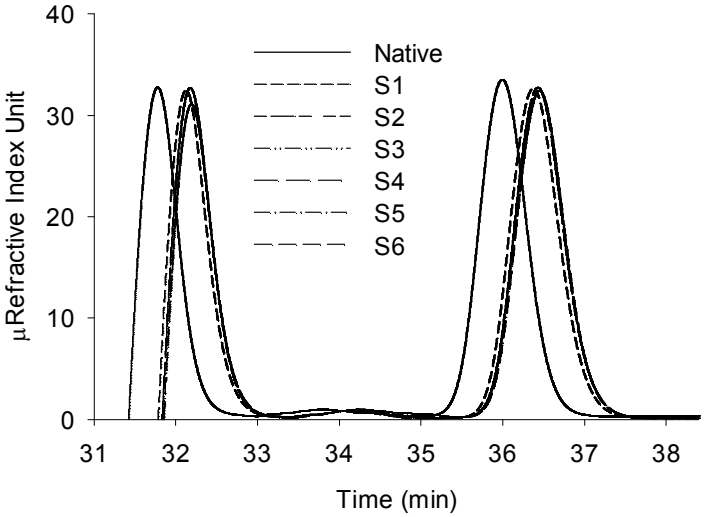

Figure 1. Comparison of the retention time of the peaks in gel permeation chromatography of starch samples.

Table 1. Peak retention time of native and sonicated high-amylose corn starch.

Sample[1)]	Percent retention time (min)	
	Peak I[2)]	Peak II[3)]
Native	31.78	35.99
S1	32.12	36.37
S2	32.13	36.37
S3	32.18	36.43
S4	32.18	36.43
S5	32.18	36.45
S6	32.18	36.45

[1)] Native = native high-amylose corn starch; S1-6 = starches sonicated for 10-60 min at 10 min interval.

[2)] Second eluted peak of amylose.

[3)] First eluted peak of amylopectin.

2. Proton nuclear magnetic resonance (^{1}H NMR) spectra

To further investigate the structural properties of sonicated starches, their ratio of α-1,4 and α-1,6 linkages were determined using ^{1}H NMR spectroscopy (Table 2). This analysis was the firstly tried experiment in the field of sonicated starch. Percentages of α-1,4 and α-1,6 linkages were determined using the area ratios from the spectra in which peaks at 5.4 and 5.0 ppm were assigned to H-1 of α-1,4 and α-1,6 linked units, respectively (Figure 2). Panose was used as a standard to verify the positions for H-1 of α-1,4 and α-1,6 linked units since it has 50% α-1,4 and 50% α-1,6 linkages. Proportions of α-1,4 linkage reduced slightly from 99.21% to 98.19% because of the extended sonication time. This result can be explained by Gibbs free energy difference between α-1,4 linkage (ΔG = -15.5 kJ/mol) and α-1,6 linkage (ΔG = -7.1 kJ/mol). α-1,4 Linkage is more favorable to the hydrolysis reaction (Voet et al., 2013), leading to the hydrolysis of α-1,4 linkage in α-glucans caused by both shear forces from the burst of the microbubbles and chemical reaction between starch and radicals generated from the bubble cavitation under the sonication. In addition, Fourier transform infrared spectroscopy of sonicated HACS paste showed that α-1,6 linkage was maintained under energy input of 750W at 20 kHz (Kang et al.,

2016). The decrease in the proportion of α-1,4 linkage, therefore, was not caused by hydrolysis of α-1,6 linkage, but only by hydrolysis of α-1,4 linkage, subsequently resulting in the reduction of molecular weight of starch as shown in GPC.

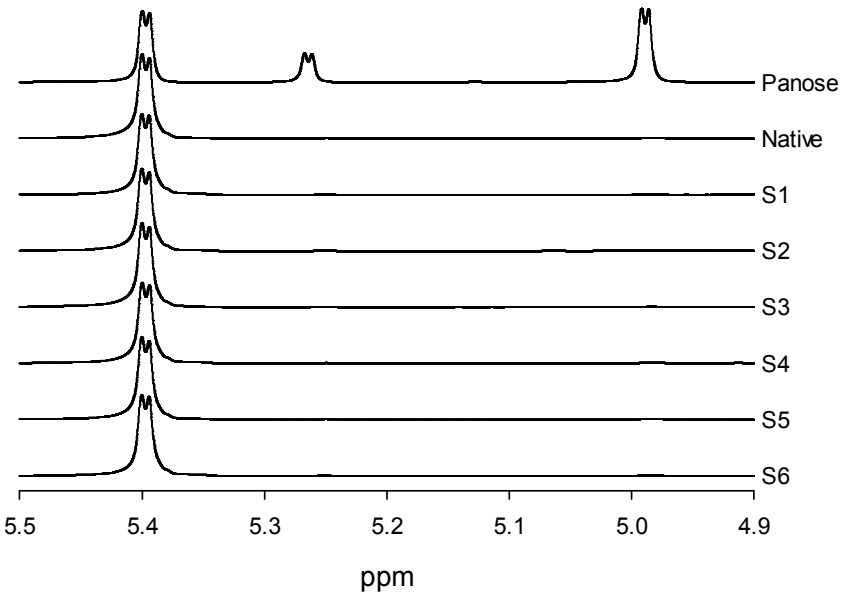

Figure 2. ^{1}H NMR spectra of native and sonicated high-amylose corn starch.

Table 2. Proportions (%) of α-1,4 and α-1,6 linkages in the starches

Sample[1)]	α-1,4 linkage	α-1,6 linkage
Panose	49.98	50.02
Native	99.21	0.80
S1	99.01	0.99
S2	98.96	1.04
S3	98.93	1.07
S4	98.81	1.19
S5	98.24	1.76
S6	98.19	1.81

[1)] Native = native high-amylose corn starch; S1-6 = starches sonicated for 10-60 min at 10 min interval.

3. Apparent amylose content

Amylose develops blue color when it forms a single helical complex with iodine (Conde-Petit et al., 1998). Apparent amylose content of native HACS (50.80%) corresponded to the information provided by its supplier, Ingredion. Apparent amylose content of sonicated starches was higher than that of native starch because the hydrolysis of α-1,4 linkage caused collapse of AM single helix, which provided more space to form a complex with iodine (I_3^-). During retrogradation, AM single helices could form the AM double helix, which acts as a crystal nucleus. Sonication raises the apparent amylose content in corn, potato, sago, and mungbean starches, which can be attributed to partial depolymerization of amylose (Chan et al., 2010; Tian et al., 2013). Though apparent amylose content increased 4.38% by 10 min sonication treatment compared to native HACS, it is revealed that sonication time affects the content slightly.

Table 3. Apparent amylose contents (%) of native and sonicated high-amylose corn starch

Sample[1)]	Amylose contents (%)
Native	50.80 ± 0.18^{c} [2) 3)]
S1	55.18 ± 0.72^{b}
S2	55.42 ± 0.42^{ab}
S3	57.22 ± 0.79^{a}
S4	56.15 ± 1.11^{ab}
S5	56.92 ± 0.10^{ab}
S6	56.57 ± 1.05^{ab}

[1)] Native = native high-amylose corn starch; S1-6 = starches sonicated for 10-60 min at 10 min interval.

[2)] Data are expressed as average value and standard deviation.

[3)] The values with different superscripts in the same column are significantly different ($p<0.05$) by Tukey's honest significant difference (HSD) test.

4. Thermal transition properties

Thermal transition properties of HACS subjected to sonication were analyzed using DSC. The onset temperature (T_o), peak temperature (T_p), conclusion temperature (T_c), and melting enthalpy (ΔH) of native and sonicated HACS are shown in Table 4. T_p represents structural stability. T_o and T_c are associated with melting of the weakest crystallites and the strongest crystallites, respectively (Barichello et al., 1990; Biliaderis et al., 1980). ΔH reflects the overall crystallinity and is an indicator of the loss of molecular order within the granule (Hoover & Vasanthan, 1994).

Three different kinds of endothermic peaks were exhibited in this study (Table 4). The first peak (peak I) indicates the melting of AP crystallites of HACS. As the sonication time increased, all the transition temperatures and ΔH of peak I decreased gradually, which showed the breakdown of the AP crystallites due to the reduction in molecular weight by sonication treatment. Furthermore, the extent of the decrease in T_c (5.68°C) was greater than that in T_o (2.86°C) leading to the reduced T_r values of all starch samples. It is could be explained by the fact that relatively stable AP crystallites remained intact during the sonication. Sonication treatment for 60 min could be considered as the time giving maximum sonication effect based on the result that S5 and S6 showed no significant difference (p<0.05).

The second peak (peak II) represents the melting of inherent AM-lipid complex present in HACS. Sonication weakened the interference between peak I and peak II, and thus T_o of peak II in sonicated starches was lower than that in native starch, because a decrease in T_c of peak I induced by sonication removed the overlap between T_c of peak I and T_o of peak II. A reduction in interference also resulted in larger ΔH and higher T_c of peak II, leading to a wider transition temperature range of sonicated starches than that of native starch. The changes in DSC parameters, thus, were caused not by the alteration of the structure but by the decrease in interference between peak I and peak II. In addition, there was no significant difference (p>0.05) in both ΔH between sonicated starches and T_p of peak II among all starch samples, and therefore the AM-lipid complex was not disrupted during the sonication.

The third peak (peak III) exhibits the melting of the AM crystallites of HACS. Sonicated starches did not have any peak III because a small quantity of AM crystallites was destroyed completely by sonication. It was in agreement with that structure of starches with a higher amount of amylose was more vulnerable to sonication (Luo et al., 2008; Zhu et al., 2012).

The glass transition temperature (T_g) of HACS was also investigated to determine the TC condition, and similar results were obtained in all samples.

DSC parameters are important for not only examination of changes in

thermal transition properties caused by sonication but also determination of TC retrogradation conditions. The condition of TC retrogradation was determined to be 4°C and 70°C, which is the temperatures near T_g and melting temperature of AP, respectively, promoting the nucleation and propagation of starch retrogradation.

Table 4. Thermal transition properties of native and sonicated high-amylose corn starch

Sample[1)]	Peak I					Peak II				Peak III				T_g(°C)
	T_o(°C)[2)]	T_p(°C)	T_c(°C)	T_r(°C)	ΔH(J/g)	T_o(°C)	T_p(°C)	T_c(°C)	ΔH(J/g)	T_o(°C)	T_p(°C)	T_c(°C)	ΔH(J/g)	
Native	71.17 ±0.17[a3)]	77.96 ±0.07[a]	87.92 ±0.51[a]	16.75 ±0.38[a]	7.64 ±0.22[a]	92.08 ±0.17[a]	97.01 ±0.09[a]	102.63 ±0.25[b]	0.50 ±0.09[b]	144.52 ±0.31	150.26 ±0.34	155.17 ±0.21	1.12 ±0.09	1.81 ±0.12[ab]
S1	69.85 ±0.42[b]	77.05 ±0.29[b]	84.09 ±0.24[b]	14.24 ±0.64[b]	5.17 ±0.19[b]	90.12 ±0.25[b]	97.52 ±0.43[a]	104.19 ±0.35[a]	1.31 ±0.10[a]	N.D.[4)]				1.77 ±0.07[b]
S2	69.95 ±0.86[b]	77.05 ±0.15[b]	83.94 ±0.33[b]	13.99 ±1.17[b]	4.62 ±0.06[bc]	90.07 ±0.16[b]	97.33 ±0.28[a]	104.45 ±0.23[a]	1.36 ±0.09[a]	N.D.				1.83 ±0.07[ab]
S3	69.34 ±0.24[bc]	76.22 ±0.33[c]	83.44 ±0.41[bc]	14.09 ±0.17[b]	4.09 ±0.31[c]	89.85 ±0.35[b]	97.09 ±0.24[a]	104.72 ±0.51[a]	1.29 ±0.09[a]	N.D.				1.81 ±0.07[ab]
S4	68.98 ±0.29[bc]	75.73 ±0.12[c]	82.83 ±0.44[bc]	13.86 ±0.55[b]	3.10 ±0.38[d]	90.08 ±0.42[b]	96.90 ±0.28[a]	104.36 ±0.38[a]	1.31 ±0.06[a]	N.D.				1.89 ±0.10[ab]
S5	68.42 ±0.10[c]	75.64 ±0.23[c]	82.51 ±0.56[c]	14.09 ±0.54[b]	2.59 ±0.16[d]	90.07 ±0.47[b]	97.28 ±0.35[a]	104.33 ±0.23[a]	1.18 ±0.08[a]	N.D.				1.75 ±0.08[b]
S6	68.31 ±0.35[c]	75.62 ±0.24[c]	82.24 ±0.67[c]	13.93 ±0.32[b]	2.56 ±0.28[d]	90.38 ±0.33[b]	97.12 ±0.26[a]	103.93 ±0.41[a]	1.27 ±0.12[a]	N.D.				1.99 ±0.06[a]

[1)] Native = native high-amylose corn starch; S1-6 = starches sonicated for 10-60 min at 10 min interval.

[2)] T_o, T_p, T_c, T_r and ΔH indicate the onset temperature, peak temperature, conclusion temperature, temperature range of crystal melting and enthalpy change of melting, respectively.

[3)] The values with different superscripts in the same column are significantly different (p<0.05) by Tukey's honest significant difference (HSD) test.

[4)] Not detected.

5. X-ray diffraction patterns and relative crystallinity

The X-ray diffraction patterns of native and sonicated HACS are displayed in Figure 3. Native HACS had strong peaks at 5.6° and 17.2°, a weaker peak at 15° and a doublet peak at 22° and 24°, thus this was B-type pattern starch. On the other hand, all major peaks of sonicated HACS showed lower intensity, and the disappearance of several peaks including 5.6° and doublet peaks suggested that sonication contributed to structural changes in starch. Sonicated starches had B-type diffraction pattern similar to native starch.

Major peak intensities were calculated to analyze the alteration of each peak (Table 5). AM and AP of various starch sources including cassava, corn, banana, and potato show their distinctive peak in XRD (Pineda-Gómez et al., 2014). The first small peak at 5.6° peak of AM crystallite disappeared due to the sonication, which was consistent with the vanishment of DSC peak III in sonicated HACS. Furthermore, likewise the decline in enthalpy of DSC peak I, the intensity of the peak at 15° decreased 1.36% in S1 and showed a gradual reduction in intensity after 20 min sonication treatment, revealing the breakdown of AP crystallites. The decrease in intensity of 17.2° peak indicates that AM double helices were collapsed significantly (Tanaka et al., 2015).

Both AM-lipid complex and AM crystallite appeared as the peak at 20°. Maintenance of AM-lipid complexes under the sonication conditions was supported by the similar peak intensities among sonicated starches and this observation corresponded with the maintenance in DSC peak II. Thus, the sonication treatment lowered the intensity of 20° peak owing to the breakdown of AM crystallites. The doublet between 22° and 24° related to the AM crystallites disappeared in sonicated HACS, it resulted in the exposure of 23° peak, which was covered by doublet. The intensity of 23° peak, indicating the AP crystallites, decreased gradually like the enthalpy of DSC peak I through the sonication as observed in acid treatment (Chung et al., 2003). Combination of the decreased tendency in each peak caused the decrement of relative crystallinity indicating the breakdown of AM and AP crystallites mentioned in DSC parameters. An increase in sonication treatment time caused a decrease in relative crystallinity by 1.47% from 50 min to 60 min treatment, and this variation was higher than that of other time intervals.

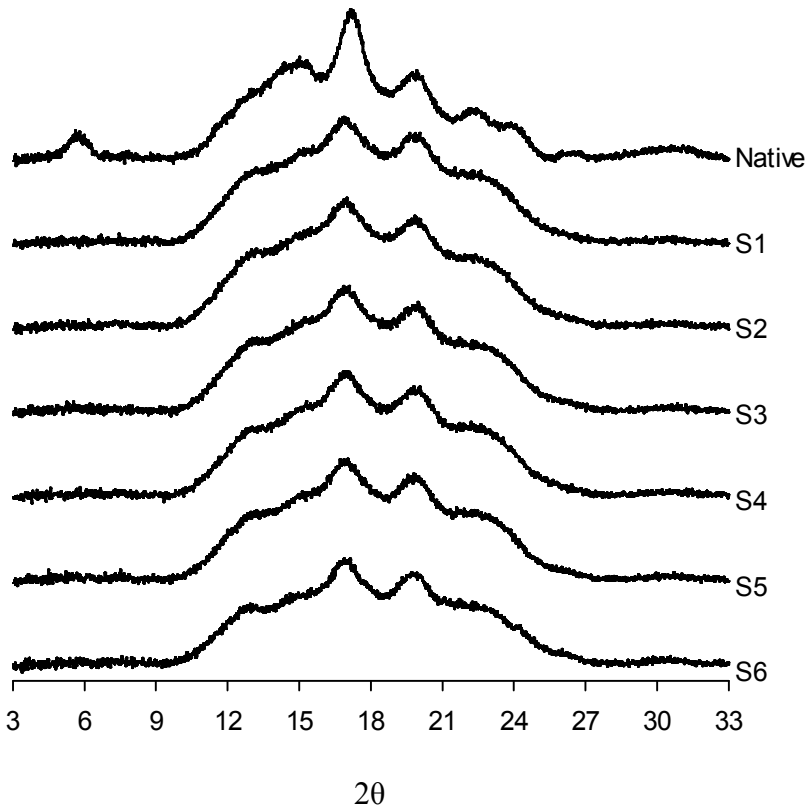

Figure 3. X-ray diffraction patterns of native and sonicated high-amylose corn starch.

Table 5. Major peak intensities and relative crystallinity of native and sonicated high-amylose corn starch

Sample[1)]	Degree of crystallinity (%)								Total crystallinity (%)
	5.6°	13°	15°	17.2°	20°	22°	23°	24°	
Native	0.48 ±0.04	3.04 ±0.05$^{a3)}$	5.11 ±0.05^{a}	8.30 ±0.02^{a}	4.72 ±0.04^{a}	2.39 ±0.03	N.D.	1.92 ±0.04	25.97±0.25^{a}
S1	N.D.[2)]	2.77 ±0.04^{b}	3.75 ±0.04^{b}	6.17 ±0.03^{b}	4.39 ±0.05^{b}	N.D.	2.55 ±0.05^{a}	N.D.	19.63±0.21^{b}
S2	N.D.	2.52 ±0.09^{c}	3.64 ±0.07^{b}	6.08 ±0.03^{b}	4.45 ±0.02^{b}	N.D.	2.44 ±0.06^{ab}	N.D.	19.13±0.25^{b}
S3	N.D.	2.34 ±0.01^{d}	3.46 ±0.01^{c}	5.96 ±0.01^{c}	4.44 ±0.03^{bc}	N.D.	2.38 ±0.12^{bc}	N.D.	18.57±0.12^{c}
S4	N.D.	2.19 ±0.04^{e}	3.32 ±0.03^{d}	5.84 ±0.04^{d}	4.42 ±0.05^{bc}	N.D.	2.25 ±0.01^{cd}	N.D.	18.03±0.15^{d}
S5	N.D.	2.11 ±0.04^{e}	3.23 ±0.03^{d}	5.74 ±0.02^{e}	4.35 ±0.01^{bc}	N.D.	2.18 ±0.02^{d}	N.D.	17.60±0.10^{d}
S6	N.D.	1.73 ±0.05^{f}	2.83 ±0.04^{e}	5.40 ±0.05^{f}	4.32 ±0.04^{c}	N.D.	1.85 ±0.02^{e}	N.D.	16.13±0.15^{e}

[1)] Native = native high-amylose corn starch; S1-6 = starches sonicated for 10-60 min at 10 min interval.

[2)] Not detected.

[3)] The values with different superscripts in the same column are significantly different (p<0.05) by Tukey's honest significant difference (HSD) test.

6. Solid-state ^{13}C cross-polarization and magic-angle spinning (CP/MAS) nuclear magnetic resonance (NMR) spectra

In ^{13}C CP/MAS NMR spectra of native and sonicated HACS, the intensity of sonicated HACS was declined as the sonication treatment time increased (Figure 4). C-1 region of the spectra including the double helical structure showed a lower intensity in the sonicated starches.

Resonance peaks in the regions 90-110, 67-90 and 58-67 ppm were assigned to C-1, C-2, -3, -4, -5 and C-6 sites, respectively (Gidley & Bociek, 1985). Gidley and Bociek (1985) showed that ^{13}C CP/MAS NMR spectra for granular starches can be interpreted as a composite of intensity features from ordered (double-helical) and non-ordered (amorphous single chain) materials. This was based primarily on chemical shift and line shape differences in C-1 and C-4 sites in double-helical and amorphous states. Resonance peaks in the regions 80–87 and 103–104 ppm are characteristic for non-double-helical (amorphous) material, while the signal at 99–102 ppm is characteristic for starch double helices (Gidley & Bociek, 1985; Gidley & Bociek, 1988; Gidley & Bulpin, 1989; Gidley et al., 1995). By comparison of the relative intensities of these signals for different samples, it is thus possible to compare the relative double-helix contents in starch samples.

In sonicated starches, relative C-1 intensity was lower in the range 99–102

and higher in the ranges 80–87 and 103–104 ppm than native starch. This indicated a lower double-helical content compared with native starch.

In addition, the proportion of ordered structure for starch samples was changed from 39.49% to 31.98% as sonication time extended (Table 6). It was in accordance with the results of thermal transition properties and relative crystallinity analyses (Table 4 & 5). A decrease in the proportion of double-helical structure obtained by ^{13}C CP/MAS NMR was greater than that of relative crystallinity acquired by XRD. All crystallites were not detected by XRD method. It has been shown that X-ray diffraction did not detect irregularly packed structures (Gidley & Bociek, 1985). This result was in agreement with a study of acid-modified tapioca starch (Atichokudomchai et al., 2004).

In the estimation of single and double helices by ^{13}C CP/MAS NMR (Lopez-Rubio et al., 2008), double helix content of waxy maize starch (47%) was almost double compared to HYLON VII (24%). This result indicates that AP contained more double helices than AM. Thus, a 4.23% decrease in ordered structure by 10 min sonication treatment can be explained by the collapse of a relatively small quantity of AM double helix. This phenomenon was also observed in an increased retention time of AM in GPC, a decrease in the portion of α-1,4 linkage in ^{1}H NMR and an increment of apparent amylose content caused by disruption of AM double helices. In spite of those

results, all of the AM double helices were not collapsed by sonication treatment because the transition temperature of AM crystallites was above 140°C. Thus, AM double helices consisting AM crystallites were more tolerable to physical treatments including sonication than AM crystallites were. AM double helices were formed by numerous hydrogen bonds between two adjacent AM single helices, leading to enhanced resistance to sonication than AM crystallites. Therefore, AM double helices remained intact during the sonication treatment and it could be observed by the intensity of peak at 17.2° in XRD. Otherwise, all of the AM crystallites would be disappeared. These phenomena are correlated to the vanishment of peak III enthalpy in DSC, and peak at 5.6° and doublet peak at 22° and 24° in XRD, and decrease in intensity of peak at 20° during 10 min sonication treatment in XRD.

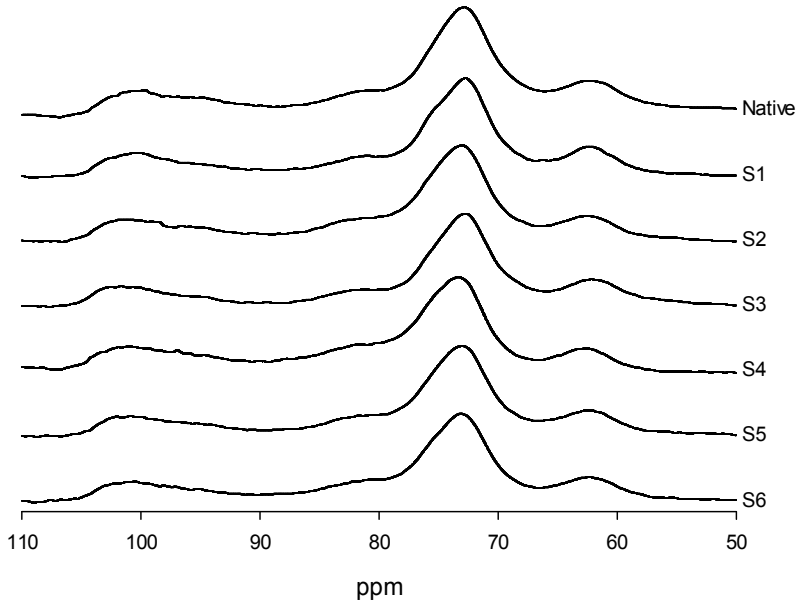

Figure 4. ^{13}C CP/MAS NMR spectra of native and sonicated high-amylose corn starch.

Table 6. The proportion of ordered structure of starches

Sample[1)]	Ordered (%)[2)]	Amorphous (%)[3)]	O/A ratio[4)]
Native	39.49	60.51	0.65
S1	35.26	64.74	0.55
S2	34.94	65.06	0.54
S3	33.92	66.08	0.51
S4	33.88	66.12	0.51
S5	32.02	67.98	0.47
S6	31.98	68.02	0.47

[1)] Native = native high-amylose corn starch; S1-6 = starches sonicated for 10-60 min at 10 min interval.

[2)] The proportion of ordered structure.

[3)] The proportion of amorphous structure.

[4)] The ratio ordered structure to amorphous structure.

7. Branched chain length distribution

The AP branched chain length distribution of native and sonicated starches are shown in Table 7. Average DP decreased gradually as time of sonication increased. Outer branched chains were vulnerable to sonication and this result can be explained by Gibbs free energy of α-1,4 (ΔG = -15.5 kJ/mol) and α-1,6 linkages (ΔG = -7.1 kJ/mol). It is well known that α-1,4 linkage is more favorable to the hydrolysis reaction causing mechanical decomposition and chemical depolymerization of α-1,4 linkage (Voet et al., 2013). However, a slight overall decline in average DP to 0.74 indicated that sonication had a little effect on outer branched AP chains.

If the hydrolysis of α-1,4 bonds by sonication could randomly occur in crystalline region of AP, a gradual decrease in average DP would not be observed. Also, average DP would decrease to a greater extent as compared with the result obtained from the present study. Thus, amorphous region of AP is expected to be the site of the α-1,4 linkage hydrolysis. Amorphous region is more susceptible to physical, chemical, and enzymatic degradation than crystalline region is (Hoover, 2000; Whistler et al., 1984). Hydrolysis of α-1,4 bonds in the amorphous region, which plays an important role in linking the AP clusters, resulted in the disintegration of AP clusters by sonication. In addition, hydrolysis of α-1,4 linkage observed in ^{1}H NMR

supports this explanation. A decrement of molecular weight of AP in GPC, the gradual breakdown of the AP crystallites as shown in DSC peak I enthalpy, and decreased peak intensities of 15° and 23° in XRD resulted from the separation of AP clusters. AM also coexists with the AP cluster, and AM random coil located at the amorphous region of cluster would be disintegrated during sonication.

Hydrolysis of α-1,4 linkage at terminal sites of branched AP chain was estimated by HPAEC, as mentioned above. Among sonicated starches, it was confirmed by the reduction of α-1,4 linkage ratio in ^{1}H NMR. Decrease in AP double helical structure observed with ^{13}C CP/MAS NMR also resulted from the hydrolysis at terminal sites. In spite of the hydrolysis at outer chains, this reaction slightly affected the decrease in molecular weight of HACS.

AP chain length is an important factor affecting the extent of retrogradation, and the chains with DP 16-24 would accelerate the retrogradation (Kaletunç & Breslauer, 2003; Ward et al., 1994; Yuryev et al., 2007). In native HACS, the proportion of DP 13-24 fraction increased from 48.56% to 49.87% after 60 min sonication. Therefore, this slight alteration of distribution would contribute to increased retrogradation, because the distribution pattern remained almost the same during the sonication due to negligible hydrolysis of α-1,4 linkages in crystalline region. Though the chain length distribution for the high extent of retrogradation could be optimized by the chemical and

enzymatic degradation, broad distribution of molecular weight would make the achievement of optimized distribution difficult (Ba et al., 2013; Nitsch, 1995).

Structural properties of native and sonicated HACS were characterized by various experiments and statistically analyzed by Tukey`s HSD test. Among sonicated HACS, S6 showed considerable differences between native HACS in various structural properties, and experimental data of XRD were significantly different (p<0.05) from the other HACSs sonicated less than 50 min. A decrease in molecular weight by sonication resulted in the reduction of relative crystallinity, and it affected the extent of decrease in the double helical structure. Imperfectness and defectiveness of the packing of the double helices within the crystallites are important factors contributing to the gelatinization (Genkina et al., 2007). Thus, native HACS and S6 were retrograded under both isothermal storage and TC conditions in Section II.

Table 7. Branched chain length distribution of native and sonicated high-amylose corn starch

Sample[1)]	Percent distribution (%)				DPn[3)]
	DP[2)] 6-12	DP 13-24	DP 25-36	DP ≥ 37	
Native	20.15±0.23^{a}[4)]	48.56±0.23^{b}	17.72±0.11^{a}	13.57±0.21^{a}	22.18±0.08^{a}
S1	20.28±0.23^{a}	48.85±0.23^{ab}	17.60±0.13^{a}	13.26±0.13^{ab}	22.07±0.03^{ab}
S2	20.43±0.08^{a}	48.98±0.16^{ab}	17.64±0.07^{a}	12.95±0.10^{abc}	21.95±0.05^{abc}
S3	20.68±0.35^{a}	49.47±0.31^{ab}	17.51±0.14^{a}	12.32±0.33^{abc}	21.72±0.12^{abc}
S4	20.90±0.72^{a}	49.83±0.20^{a}	17.31±0.50^{a}	11.93±0.08^{bc}	21.56±0.12^{bc}
S5	21.09±0.62^{a}	49.64±0.56^{ab}	17.19±0.33^{a}	12.08±0.66^{bc}	21.55±0.27^{bc}
S6	21.21±0.70^{a}	49.87±0.77^{a}	17.15±0.36^{a}	11.77±1.03^{c}	21.44±0.41^{c}

[1)] Native = native high-amylose corn starch; S1-6 = starches sonicated for 10-60 min at 10 min interval.

[2)] DP, degree of polymerization.

[3)] Number-based average degree of polymerization.

[4)] The values with different superscripts in the same column are significantly different (p<0.05) by Tukey's honest significant difference (HSD) test.

8. Principal component analysis of structural properties in relation to sonication treatment

Principal component analysis (PCA) was conducted to summarize the results from structural properties induced by sonication (Figure 5). PCA loading plots provided an overview of the similarities and differences among sonication treatment conditions based on the relationships underlying the measured structural characteristics. The first and second principal components (PCs) could describe 54.97% and 42.31% of total variance, respectively, indicating that the first two PCs explained most of the variability underlying the experimental data. PC1 was majorly defined by the presence of sonication and the properties driven by the sonication, while PC2 could be defined by sonication time and the properties differentiated by the treatment time.

High positive correlation was indicated among peak intensity (13°, 15°, 17.2°, and 20°), relative crystallinity, average DP, O/A ratio, proportion of ordered structure, thermal properties (T_c, T_o, T_p, T_r, and ΔH) and concentration of α-1,4 linkages loaded positively on PC1. Native HACS was loaded close to these properties indicating that these attributes were strong in native starch. Sonicated starches were located close each other along with retention time of AM and AP, concentration of α-1,6 linkages, AAC and

proportion of amorphous structure loaded negatively on PC1 indicating that these attributes were strong in sonicated samples (Tables 1, 3 and 6).

Native HACS and sonicated starches treated less than 30 min were located positively on PC2 along with high relative crystallinity and properties driven by high crystalline structure, peak intensity (13°, 15°, 17.2°, and 20°), relative crystallinity, average DP, O/A ratio, proportion of ordered structure, thermal properties (T_c, T_o, T_p, T_r, and ΔH) and concentration of α-1,4. Retention time of AM and AP, concentration of α-1,4 linkages, AAC and proportion of amorphous structure were highly loaded on PC2 in the negative direction where S4, S5 and S6 were located, demonstrating that these attributes were strong in samples with sonication over 40 min.

In summary, PCA loading plot clearly manifested the effects of sonication which are a decrease in molecular weight, collapse of AM double helices, breakdown of starch crystallite, reduction in outer branched chain length, and hydrolysis of α-1,4 glycosidic bonds.

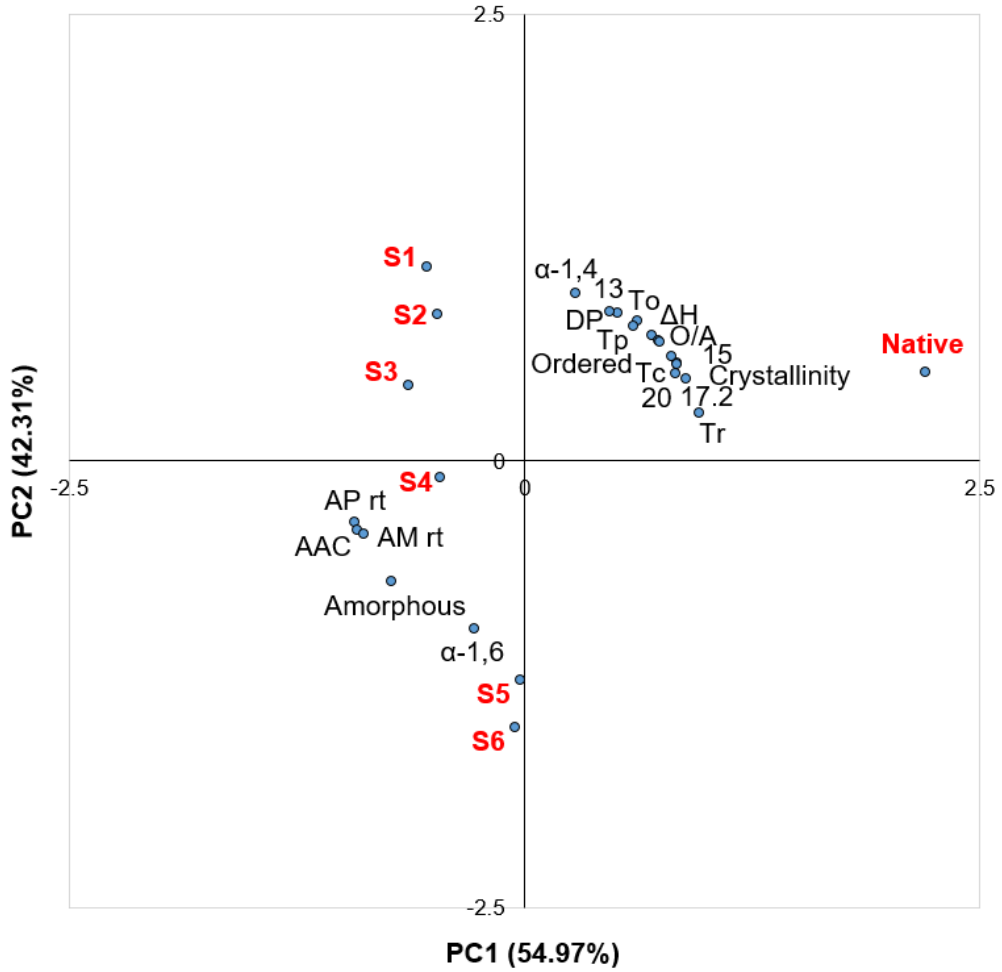

Figure 5. Principal component loading plot of PC1 and PC2 describing the variation among properties of sonicated starches.

13: peak intensity of 13°; 15: peak intensity of 15°; 17.2: peak intensity of 17.2°; 20: peak intensity of 20°; AAC: apparent amylose content; AM rt: retention time of amylose; Amorphous: proportion of amorphous structure; AP rt: retention time of amylopectin; Crystallinity: relative crystallinity; DP: average degree of polymerization; O/A: ratio of ordered structure to amorphous structure; Ordered: proportion of ordered structure; T_c: conclusion temperature; T_o: onset temperature; T_p: peak temperature; T_r: temperature range of crystal melting; α-1,4: concentration of α-1,4 linkages; α-1,6: concentration of α-1,6 linkages; *ΔH*: enthalpy change of melting; Native = native high-amylose corn starch; S1-6 = starches sonicated for 10-60 min at 10 min interval.

[Section II] Retrogradation properties of native and sonicated HACS treated with isothermal storage and temperature-cycling

1. Sources in F-table

All experimental data in section II was analyzed using Tukey`s HSD test and the significance level is shown in Table 8. The factors of 3-way MANOVA were presence of sonication, retrogradation period (0, 4, 8, 12, 16, and 60 d), and storage type (gelatinization, isothermal storage, temperature-cycling, and long-term storage). The interactions of 2 factors each (presence of sonication * retrogradation period, retrogradation period * storage type, and presence of sonication * storage type) were also applied to analysis.

From the viewpoint of statistics, 6 sources in F-table would affect the retrogradation of starch. First, presence of sonication affected the nucleation step because of the collapse of AM double helix and a decrease in molecular weight of AP by sonication made dense arrangement of AP and an increased degree of retrogradation (Chang & Lin, 2007; Harder et al., 2015). Secondly, longer period of retrogradation resulted in the formation of more perfect crystallites of starch (Ambigaipalan et al., 2013). Thirdly, storage type of temperature-cycling was accompanied with both nucleation and propagation,

which occurred near T_g and melting temperature, respectively. Therefore, overall crystallization of starch in TC was higher than in isothermal storage.

In addition, interaction of two factors was applied to the MANOVA. First, the interaction between sonication and retrogradation period suggested that the conformation change of AM random coil to AM single helix by coil-to-helix transition might occur during the storage, followed by hydrolysis of AM single helix and random coil by sonication (Heineck et al., 2008). AM single helices form AM double helix, performing as AM nuclei in the nucleation stage of retrogradation. Though AP crystallization is slow and takes a few weeks (Van Soest et al., 1994), reduced molecular weight of AP by sonication accelerates the retrogradation process of AP. Secondly, a significant interaction of retrogradation and storage type indicated that more perfect crystallites were formed during longer-time isothermal storage, and repeated nucleation and propagation of longer-storage temperature-cycling caused a high degree of retrogradation. Finally, the interaction between sonication and storage type suggested that repetition of nucleation during the second cycle of temperature-cycling induced higher nucleation of AM. Propagation during temperature-cycling and dense arrangement of AP by sonication also could promote the retrogradation of AP.

All the coefficients of determination (R^2) of experimental data of retrograded starch were above 0.95 (Table 8). The treatment conditions set

for retrogradation could explain more than 95% extent in the whole range of DSC, XRD parameters and RS contents caused by retrogradation.

Table 8. F-table

Source	Significance level							
	DSC ΔH [1)]		XRD[2)]					RS content[3)]
	Peak I	Peak III	13°	17.2°	20°	23°	Relative crystallinity	
Presence of sonication	.001	.000	.000	.000	.000	.000	.000	.000
Retrogradation period	.000	.000	.000	.000	.000	.000	.000	.000
Storage type	.000	.000	.000	.000	.000	.000	.000	.000
Presence of sonication * Retrogradation period	.555	.329	.000	.001	.000	.028	.002	.002
Retrogradation period * Storage type	.455	.742	.000	.042	.000	.772	.028	.019
Presence of sonication * Storage type	.290	.774	.734	.004	.000	.603	.000	.000
R^2 [4)]	.968	.982	.995	.997	.997	.989	.997	.990
(adjusted) [5)]	(.957)	(.976)	(.993)	(.996)	(.996)	(.985)	(.996)	(.986)

[1)] DSC, differential scanning calorimeter.

[2)] XRD, X-ray diffraction.

[3)] RS content, resistant starch content.

[4)] R^2, coefficient of determination.

[5)] Adjusted R^2, adjusted coefficient of determination.

2. Thermal transition properties

Thermal transition properties of retrograded samples were determined using DSC (Table 9 and 10). In N-0 and S6-0 (gelatinized samples), peak I was not detected due to the fully gelatinized AP crystallite, and it led to removal of interference between peak I and peak II, which was originally present in native HACS, completely. Peak II of AM-lipid complex formed by hydrophobic interaction remained under the gelatinization process in both samples. Transition temperatures and enthalpy for peak III of gelatinized samples increased compared with native and sonicated HACS (Table 4). AM crystallites would not be melted fully by boiling and autoclaving, because AM crystallites had transition temperatures above 140°C as mentioned before. Though both samples were lyophilized immediately after gelatinization, peak III was present in the N-0 and S6-0. During the temperature drop in the freezing process, these samples passed through the temperature near Tg, where nucleation of AM is accelerated. Thus, peak III was regenerated inevitably due to the strong tendency to retrograde of AM (Wang et al., 2015).

In retrograded samples, peak I shifted to lower temperature than native and sonicated HACS because gelatinization weakened the starch crystallites prior

to retrogradation. Regeneration of peak I, vanished in gelatinized samples, however, indicated AP retrogradation. Furthermore, enthalpy of peak III in retrograded samples was higher than that of gelatinized samples, and a decrease in T_c - T_o showed the production of stable AM crystallites. Peak II of AM-lipid complex was maintained during retrogradation (Zhou et al., 2013).

Enthalpy of S6-0, treated harshly with sonication and gelatinization, was the lowest among all starch samples. On the other hand, S6-I and S6-TC groups showed notably higher enthalpy in peak I and peak III than N-I and N-TC groups did, because retrogradation was promoted by the decreased molecular weight of starch due to sonication treatment. Higher increase of enthalpy in peak III than that in peak I resulted from the strong tendency of retrogradation in AM crystallites.

Collapse of AM double helices by sonication, observed in Section I, induced the increase in the number of AM nuclei, which contributed to the increase in the nucleation of starch retrogradation at 4°C near glass transition temperature (Kitamura et al., 1994). Nucleation is the rate limiting step of starch retrogradation (Arık Kibar et al., 2011), thus the acceleration of nucleation would overcome the rate limiting step and raise the overall retrogradation.

The formation of AM double helices plays an important role as AM nuclei

in nucleation (Ottenhof & Farhat, 2004). Though AM single helices and random coils were also disrupted by sonication, AM random coil changed its conformation to AM single helix by coil-to-helix transition during the storage. Thus, AM single helices would construct AM double helices, which performs as AM nuclei in nucleation of starch retrogradation. Reduction of AP molecular weight would contribute to dense arrangement of AP also and increase the retrogradation of AP. In addition, storage at 70°C in temperature-cycling accelerated the propagation of AP in retrogradation.

Enthalpy of TC retrogradation sample was higher than that of isothermal storage sample when compared within the same period of retrogradation. Repeated nucleation and propagation of TC retrogradation resulted in the formation of more perfect starch crystallites, but the degree of increment in enthalpy gradually reduced as the storage time increased. Furthermore, both native HACS and S6 showed almost the same enthalpy in retrogradation for 60 days, thus it seemed that sonication caused the acceleration of retrogradation and did not increase the degree of retrogradation. It corresponded to the results that transition enthalpy increased progressively with storage time until a certain limit was reached and remained constant on further storage (Eliasson & Gudmundsson, 2006).

The sum of enthalpy in each samples revealed an increase with retrogradation period. To understand the effects of sonication and

temperature-cycling on retrogradation, enthalpies assorted by 4 groups (N-I, N-TC, S6-I, S6-TC) were plotted by Avrami kinetics model and irreversible consecutive reaction model as follows (Figure 6 and 7). The rate of overall retrogradation could be calculated from the Avrami kinetics model. Especially, in irreversible consecutive reaction model, the rate of both nucleation and propagation was revealed.

Table 9. Thermal transition properties of retrograded native high-amylose corn starch

Sample[1)]	Peak I				Peak II				Peak III			
	T_o(°C)[2)]	T_p(°C)	T_c(°C)	ΔH(J/g)	T_o(°C)	T_p(°C)	T_c(°C)	ΔH(J/g)	T_o(°C)	T_p(°C)	T_c(°C)	ΔH(J/g)
N-0	N.D.[3)]				90.68 ±0.37^{ab}	97.17 ±0.39^{ab}	104.00 ±0.20^{ab}	1.04 ±0.07^{a}	150.59 ±0.51^{bcde}	152.81 ±0.34^{abc}	159.45 ±0.78^{a}	1.97 ±0.31^{l}
N-I4	52.46 ±0.54^{ab}[4)]	59.74 ±0.69^{abc}	73.41 ±0.95^{ab}	1.19 ±0.13^{e}	90.57 ±0.49^{b}	96.82 ±0.35^{ab}	103.70 ±0.44^{ab}	1.10 ±0.06^{a}	150.28 ±0.72^{bcd}	152.54 ±0.42^{abc}	156.77 ±0.31^{bc}	3.65 ±0.20^{k}
N-I8	52.67 ±0.93^{ab}	59.97 ±0.48^{abc}	72.44 ±0.68^{ab}	2.95 ±0.24^{d}	90.74 ±0.45^{ab}	97.20 ±0.63^{ab}	104.13 ±0.48^{ab}	1.20 ±0.17^{a}	149.58 ±0.66^{e}	151.96 ±0.53^{bc}	157.21 ±0.40^{bc}	5.44 ±0.25^{ghi}
N-I12	52.40 ±0.68^{ab}	59.84 ±0.55^{abc}	72.54 ±0.87^{ab}	3.60 ±0.19^{bcd}	90.07 ±0.23^{b}	96.37 ±0.51^{b}	104.31 ±0.59^{ab}	1.26 ±0.12^{a}	151.50 ±0.38^{abcd}	152.16 ±0.22^{bc}	157.15 ±0.34^{bc}	7.08 ±0.29^{cde}
N-I16	53.06 ±0.19^{a}	59.93 ±0.52^{abc}	72.70 ±0.47^{ab}	4.04 ±0.28^{ab}	90.98 ±0.15^{ab}	96.91 ±0.56^{ab}	104.05 ±0.24^{ab}	1.23 ±0.10^{a}	151.81 ±0.43^{abc}	152.24 ±0.50^{bc}	156.78 ±0.62^{bc}	7.84 ±0.23^{abcd}
N-TC4	52.72 ±0.29^{ab}	59.98 ±0.52^{abc}	73.19 ±0.67^{ab}	1.35 ±0.12^{e}	90.67 ±0.34^{ab}	97.09 ±0.28^{ab}	103.85 ±0.43^{ab}	1.10 ±0.06^{a}	150.23 ±0.32^{de}	152.61 ±0.45^{abc}	157.34 ±0.58^{bc}	4.15 ±0.19^{ijk}
N-TC8	53.09 ±0.08^{a}	60.81 ±0.49^{a}	71.94 ±0.52^{b}	3.22 ±0.27^{cd}	91.14 ±0.33^{ab}	96.50 ±0.65^{b}	103.96 ±0.35^{ab}	1.21 ±0.09^{a}	150.11 ±0.71^{de}	152.19 ±0.12^{bc}	156.80 ±0.48^{bc}	5.83 ±0.20^{fgh}
N-TC12	52.73 ±0.41^{ab}	60.38 ±0.05^{abc}	72.40 ±0.54^{ab}	4.09 ±0.20^{ab}	90.15 ±0.42^{b}	97.12 ±0.60^{ab}	103.84 ±0.28^{ab}	1.09 ±0.12^{a}	151.97 ±0.46^{ab}	152.52 ±0.15^{abc}	156.38 ±0.63^{c}	7.34 ±0.27^{bcde}
N-TC16	53.16 ±0.62^{a}	60.28 ±0.10^{abc}	72.83 ±0.34^{ab}	4.27 ±0.18^{ab}	91.16 ±0.22^{ab}	96.71 ±0.50^{ab}	104.68 ±0.35^{a}	1.12 ±0.14^{a}	151.21 ±0.26^{abcd}	152.30 ±0.43^{bc}	156.81 ±0.58^{bc}	8.30 ±0.38^{ab}
N-∞	53.23 ±0.49^{a}	60.91 ±0.65^{abc}	72.25 ±0.16^{ab}	4.86 ±0.20^{ab}	91.28 ±0.93^{ab}	97.20 ±0.37^{ab}	104.21 ±0.39^{a}	1.15 ±0.08^{a}	151.64 ±0.53^{abcd}	152.02 ±0.15^{bc}	157.16 ±0.44^{bc}	9.13 ±0.29^{ab}

[1)] N-0=gelatinized native high-amylose corn starch; N-I/TC4-16=native high-amylose corn starches stored in isothermal condition (I) at 4°C and temperature-cycling condition (TC) 4°C and 70°C for 4-16 days at 4 days interval; N-∞=native high-amylose corn starch stored at 4°C for 60 days.

[2)] T_o, T_p, T_c and ΔH indicate the onset temperature, peak temperature, conclusion temperature, and enthalpy change of melting, respectively.

[3)] Not detected.

[4)] The values with different superscripts in the same column are significantly different (p<0.05) by Tukey's honest significant difference (HSD) test.

Table 10. Thermal transition properties of retrograded S6

Sample[1)]	Peak I				Peak II				Peak III			
	T_o(°C)[2)]	T_p(°C)	T_c(°C)	ΔH(J/g)	T_o(°C)	T_p(°C)	T_c(°C)	ΔH(J/g)	T_o(°C)	T_p(°C)	T_c(°C)	ΔH(J/g)
S6-0	N.D.[3)]				90.65 ±0.44^{ab}	97.04 ±0.30^{ab}	103.84 ±0.37^{ab}	1.08 ±0.05^{a}	151.26 ±0.40^{abcd}	152.67 ±0.46^{abc}	158.54 ±0.64^{ab}	1.66 ±0.25^{l}
S6-I4	52.57 ±0.70^{ab}[4)]	59.80 ±0.55^{abc}	73.77 ±0.64^{a}	1.32 ±0.21^{e}	91.03 ±0.76^{ab}	96.36 ±0.51^{b}	104.11 ±0.63^{ab}	1.25 ±0.15^{a}	150.12 ±0.29^{de}	153.75 ±0.47^{a}	157.43 ±0.89^{bc}	4.49 ±0.35^{ijk}
S6-I8	52.24 ±0.52^{ab}	60.41 ±0.72^{ab}	72.97 ±0.43^{ab}	3.11 ±0.38^{cd}	90.31 ±0.91^{b}	96.80 ±0.58^{ab}	103.99 ±0.27^{ab}	1.23 ±0.08^{a}	150.68 ±0.49^{abcde}	152.12 ±0.17^{bc}	157.11 ±0.24^{bc}	6.38 ±0.62^{efg}
S6-I12	53.13 ±0.30^{a}	59.15 ±0.29^{bc}	73.15 ±0.60^{ab}	3.79 ±0.30^{bc}	90.04 ±0.55^{b}	96.42 ±0.06^{b}	104.44 ±0.75^{ab}	1.18 ±0.19^{a}	151.67 ±0.33^{abcd}	152.36 ±0.68^{bc}	157.70 ±0.39^{abc}	7.77 ±0.56^{abcd}
S6-I16	52.55 ±0.70^{ab}	60.12 ±0.40^{abc}	72.30 ±0.44^{ab}	4.15 ±0.07^{ab}	91.59 ±0.25^{ab}	97.11 ±0.23^{ab}	103.46 ±0.63^{ab}	1.23 ±0.12^{a}	151.40 ±0.85^{abcd}	151.94 ±0.13^{bc}	157.39 ±0.32^{bc}	8.53 ±0.29^{a}
S6-TC4	52.29 ±0.48^{ab}	60.28 ±0.15^{abc}	72.72 ±0.60^{ab}	1.54 ±0.33^{e}	91.17 ±0.72^{ab}	96.76 ±0.36^{ab}	104.19 ±0.20^{ab}	1.22 ±0.14^{a}	150.13 ±0.28^{de}	153.18 ±0.22^{ab}	156.91 ±0.63^{bc}	5.05 ±0.46^{hij}
S6-TC8	52.79 ±0.83^{ab}	60.21 ±0.10^{abc}	72.77 ±0.39^{ab}	3.85 ±0.23^{abc}	92.18 ±0.70^{a}	96.87 ±0.41^{ab}	103.19 ±0.43^{b}	1.18 ±0.26^{a}	151.21 ±0.38^{abcd}	152.92 ±0.30^{abc}	157.13 ±0.72^{bc}	6.83 ±0.15^{def}
S6-TC12	51.06 ±0.75^{b}	59.01 ±0.34^{c}	71.83 ±0.66^{b}	4.16 ±0.09^{ab}	90.89 ±0.61^{ab}	98.03 ±0.24^{a}	102.97 ±0.82^{b}	1.26 ±0.15^{a}	152.20 ±0.31^{a}	153.19 ±0.50^{ab}	156.91 ±0.84^{bc}	8.06 ±0.10^{abc}
S6-TC16	52.66 ±0.45^{ab}	59.84 ±0.61^{abc}	72.23 ±0.18^{ab}	4.50 ±0.32^{a}	90.83 ±0.57^{ab}	97.05 ±0.40^{ab}	104.11 ±0.76^{ab}	1.09 ±0.06^{a}	151.55 ±0.71^{abcd}	151.80 ±0.60^{c}	156.88 ±0.51^{bc}	8.62 ±0.30^{a}
S6-∞	52.15 ±0.36^{ab}	60.07 ±0.29^{abc}	72.34 ±0.59^{ab}	4.71 ±0.16^{a}	91.75 ±0.27^{ab}	97.16 ±0.45^{ab}	104.27 ±0.76^{ab}	1.12 ±0.07^{a}	151.86 ±0.49^{abcd}	152.73 ±0.86^{c}	157.18 ±0.26^{bc}	9.18 ±0.21^{a}

[1)] S6-0=gelatinized starch after 60 min sonication; S6-I/TC4-16=60 min sonicated starches stored in isothermal condition (I) at 4°C and temperature-cycling condition (TC) of 4°C and 70°C for 4-16 days at 4 days interval; S6-∞=60 min sonicated starch stored at 4°C for 60 days.

[2)] T_o, T_p, T_c and ΔH indicate the onset temperature, peak temperature, conclusion temperature, and enthalpy change of melting, respectively.

[3)] Not detected.

[4)] The values with different superscripts in the same column are significantly different (p<0.05) by Tukey's honest significant difference (HSD) test.

2.1. Avrami kinetics model

Avrami kinetics model premises that crystals nucleate and grow until the crystallinity levels off to a constant value. Two parameters are taken in this equation. First, rate constant (*k*) containing quantitative information indicates the overall crystallization rate because both crystal nucleation and growth rates affect rate constant. Second, Avrami exponent (*n*) including qualitative information depends on two factors: type of crystal nucleation (instantaneous and sporadic) and the dimensions in which crystal growth takes place (one dimension: rod-like crystal; two dimensions: disc-like crystal; three dimensions: spherulitic crystal) (McIver et al., 1968). Starch retrogradation generally results in the n=1 type of rod-like crystal growth from instantaneous nuclei (Zhang & Jackson, 1992).

Rate constant (*k*) of N-TC and S6-TC group was higher that of N-I and S6-I group, respectively, because the temperature-cycling condition accelerated retrogradation to a greater extent compared with isothermal storage (Table 11). S6-I and S6-TC groups, which were affected by the increase in nucleation and AP retrogradation due to the reduction of molecular weight by sonication, also showed higher *k* than N-I and N-TC groups did. In addition, the difference of *k* between retrograded native HACS and S6 group was

greater in TC groups than in isothermal storage groups, because propagation is related to the retrogradation of AP. Comprehensively, *k* of S6-TC group, treated by both sonication and TC, was the highest among the four groups.

Avrami exponent (*n*) of all groups was close to 1, which showed rod-like crystal growth from instantaneous nuclei, like as in previous studies (Zhang et al., 2015; Zhang & Jackson, 1992). Although lower *n* values in S6 groups meant more instantaneous retrogradation, the change in *n* was quite small. Avrami exponent only contains qualitative information (Zhang & Jackson, 1992), and thus rate constant including quantitative information should be regarded as a significant parameter in this study.

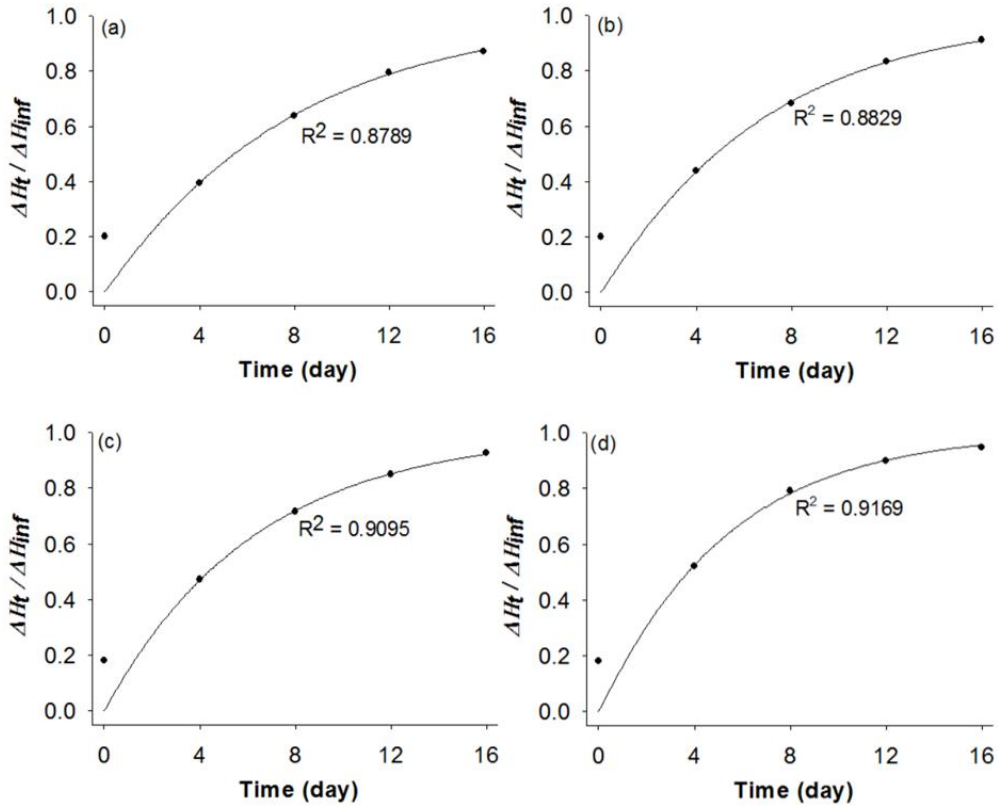

Figure 6. Plotting of Avrami kinetics model. (a) N-I group (b) N-TC group (c) S6-I group, and (d) S6-TC group.

2.2. Irreversible consecutive reaction model

Retrogradation is irreversible reaction in series. Assuming that the retrogradation is considered as consecutive unimolecular type first-order reactions, the following scheme can be suggested for the retrogradation of starch:

$$\text{Gelatinized starch} \xrightarrow{k_1} \text{Amylose nuclei} \xrightarrow{k_2} \text{Retrograded starch.}$$

$k_1 \ll k_2$, because nucleation is the rate limiting step, and then the equation (1) reduces to:

$$\Delta H_t = \Delta H_g(1 - e^{-k_1 t}).$$

This equation is identical to the Avrami equation with n=1 and indicates that rate limiting step determines the overall reaction rates. ΔH_t varies exponentially with time and reaches a constant value of ΔH_∞ as $t \to \infty$. In the analysis of data by DSC, the usual practice is to use ΔH_∞ instead of ΔH_g.

Nucleation rate constant (k_1) of four groups had a slightly higher value than the rate constant in Avrami kinetics model, but effects of sonication and temperature-cycling was identically observed in irreversible consecutive reaction model (Table 11). Much lower k_1 than propagation rate constant (k_2) indicated that nucleation was the rate limiting step of the retrogradation. Reduction of AM molecular weight by sonication treatment made k_1

increase in S6-I and S6-TC groups compared with N-I and N-TC groups. Besides, repeated nucleation in temperature-cycling resulted in higher k_1 in TC groups than isothermal storage groups.

k_2 was more than $1.0 \cdot 10^{13}$, and repeated propagation in temperature-cycling caused higher k_2 value in TC groups. Furthermore, k_2 was higher in S6 group owing to the reduced molecular weight of AP. The increment in TC groups doubled that in isothermal storage groups. It resulted from the propagation, which was mainly affected by retrogradation of AP. Avrami kinetics model could be supplemented by the irreversible consecutive reaction model.

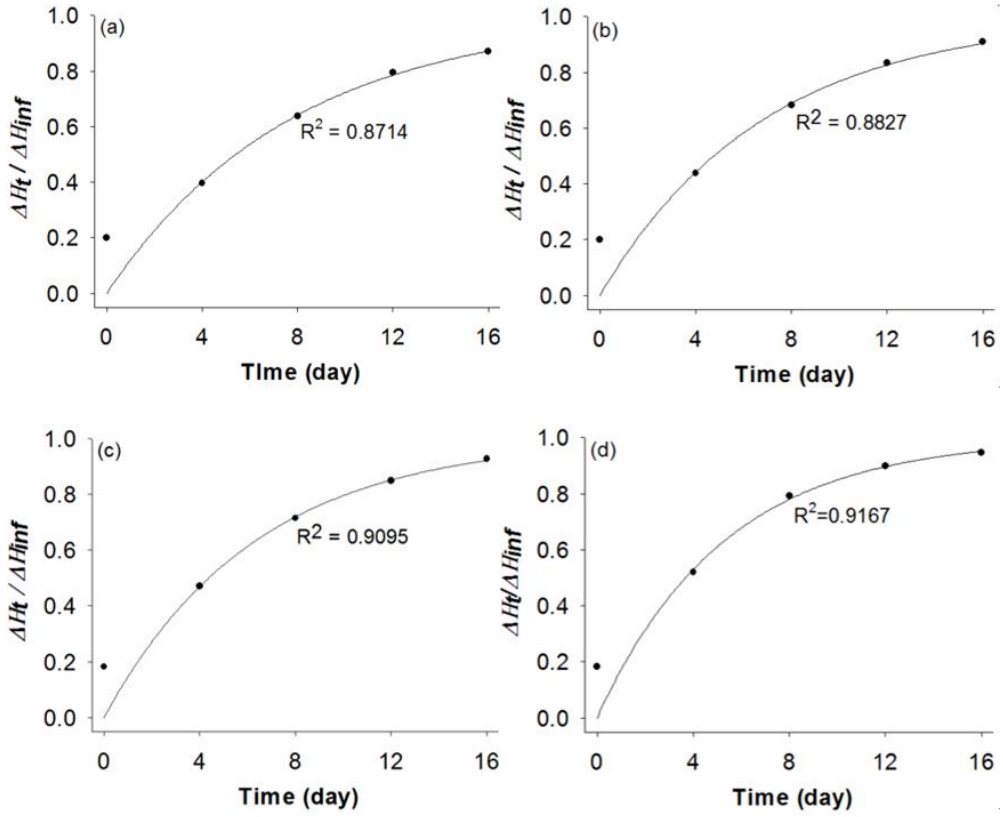

Figure 7. Plotting of irreversible consecutive reaction model. (a) N-I group (b) N-TC group (c) S6-I group, and (d) S6-TC group.

Table 11. Parameters of Avrami kinetics model and irreversible consecutive reaction model

Group[1)]	$k \cdot 10^2$ (day^{-1})	n	$k_1 \cdot 10^2$ (day^{-1})	k_2 (day^{-1})
N-I	12.11	1.0260	12.81	$1.0 \cdot 10^{13}$
N-TC	13.66	1.0317	14.59	$1.3 \cdot 10^{13}$
S6-I	15.74	1.0031	15.84	$1.1 \cdot 10^{13}$
S6-TC	17.81	1.0308	18.89	$1.5 \cdot 10^{13}$

[1)] N-I/TC=group of native high-amylose corn starches stored in isothermal condition at 4°C and temperature-cycling condition, respectively; S6-I/TC=group of 60 min sonicated starches stored in isothermal condition at 4°C and temperature-cycling condition, respectively.

3. X-ray diffraction patterns and relative crystallinity

The XRD patterns of retrograded HACS and S6 samples are displayed in Figure 8. All the samples showed B-type pattern typical for retrograded starches (Park et al., 2009).

The small 5.6° peak, disappeared in the sonicated (Figure 3) and gelatinized starches (N-0, S6-0), appeared in the samples more than 12 days retrograded S6. This remarkable phenomenon resulted from the regeneration of AM crystallites during retrogradation because small molecular weight AM, induced by sonication treatment, caused more perfect retrogradation. Also, retrograded S6 starches had about 2~3 % higher relative crystallinity when compared with the retrograded HACS under the same storage conditions. Furthermore, owing to the repeated nucleation and retrogradation, TC retrogradation samples showed higher relative crystallinity than isothermal samples did. The longer the samples were stored, the higher the relative crystallinity was.

To further analyze the alteration of peak intensities, intensities of major peak calculated are shown in Table 12. Here, the intensity of 5.6° peak was so weak that it could not be detected by the ProFit software. The crystallinity of S6-0 was the lowest among all the samples due to both sonication and gelatinization treatments.

A similar tendency of relative crystallinity related to the presence of sonication, type of storage and retrogradation period, described above, was also observed in the major peak intensities. An increase in the intensity of 17.2° peak indicated that AM double helices collapsed by sonication were regenerated during storage. The AM double helix was more actively formed in retrograded S6 sample, because disrupted AM random coil and AM single helix were united to AM double helix. It contributed to the increase in the nucleation, which is the rate limiting step of retrogradation. AM and AP crystallites also grew during storage. It was supported by the increase in the intensities of 20° and 23° peaks, corresponding to the increment of enthalpy in DSC peak I and III, which means the AM and AP crystallites, respectively.

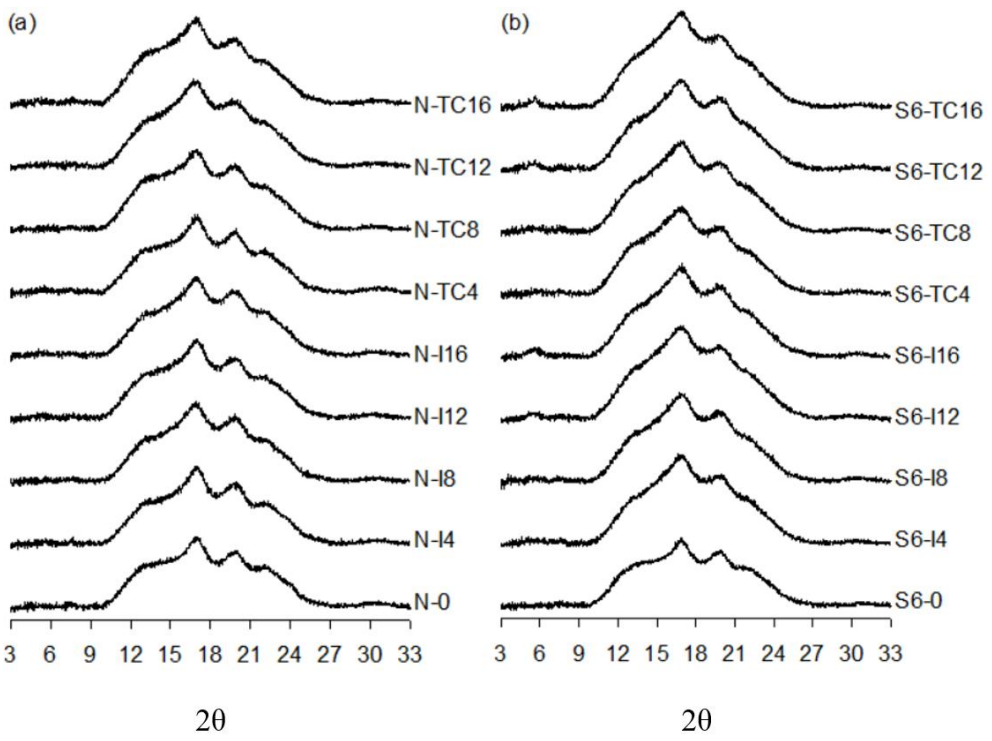

Figure 8. X-ray diffraction patterns of (a) retrograded HACS=retrograded high-amylose corn starch and (b) retrograded S6=retrograded 60 min sonicated starch.

Table 12. Major peak intensities and relative crystallinity of retrograded starches

Sample[1)]	Degree of crystallinity (%)				Total crystallinity (%)
	13°	17.2°	20°	23°	
N-0	2.76 ±0.04$^{k2)}$	4.45 ±0.03^{k}	3.45 ±0.06^{k}	2.51 ±0.04^{l}	13.17±0.15^{k}
N-I4	3.19 ±0.05^{j}	5.32 ±0.05^{j}	4.24 ±0.09^{j}	2.85 ±0.07^{k}	15.60±0.26^{j}
N-I8	3.53 ±0.04^{i}	5.65 ±0.02^{i}	4.45 ±0.03^{i}	3.37 ±0.03^{i}	17.00±0.10^{i}
N-I12	4.10 ±0.05^{g}	6.30 ±0.03^{g}	4.90 ±0.04^{h}	3.57 ±0.04^{h}	18.87±0.15^{g}
N-I16	4.61 ±0.04^{cd}	6.77 ±0.04^{ef}	5.33 ±0.08^{ef}	3.76 ±0.01^{fgh}	20.47±0.11^{e}
N-TC4	3.45 ±0.06^{i}	5.66 ±0.08^{i}	4.30 ±0.03^{ij}	3.16 ±0.09^{j}	16.57±0.25^{i}
N-TC8	3.99 ±0.06^{gh}	6.09 ±0.07^{h}	4.75 ±0.07^{h}	3.31 ±0.06^{ij}	18.13±0.25^{h}
N-TC12	4.60 ±0.03^{cd}	6.69 ±0.04^{f}	5.17 ±0.04^{fg}	3.77 ±0.05^{efg}	20.23±0.15^{e}
N-TC16	4.83 ±0.03^{b}	6.93 ±0.01^{d}	5.45 ±0.03^{e}	3.89 ±0.04^{ef}	21.10±0.10^{d}
S6-0	2.37 ±0.10^{l}	3.94 ±0.10^{l}	3.14 ±0.10^{l}	1.99 ±0.13^{m}	11.43±0.40^{l}
S6-I4	3.90 ±0.02^{h}	5.79 ±0.02^{i}	4.84 ±0.03^{h}	3.68 ±0.04^{gh}	18.20±0.10^{h}
S6-I8	4.28 ±0.02^{f}	6.35 ±0.02^{g}	5.35 ±0.06^{ef}	3.96 ±0.06^{e}	19.93±0.15^{ef}
S6-I12	4.48 ±0.02^{de}	6.90 ±0.06^{de}	5.66 ±0.07^{d}	4.35 ±0.06^{cd}	21.40±0.20^{cd}
S6-I16	4.83 ±0.08^{b}	7.37 ±0.06^{b}	6.03 ±0.06^{c}	4.64 ±0.07^{ab}	22.87±0.25^{b}
S6-TC4	4.42 ±0.04^{ef}	6.33 ±0.04^{g}	5.09 ±0.03^{g}	3.69 ±0.04^{gh}	19.53±0.15^{f}
S6-TC8	4.72 ±0.06^{bc}	6.80 ±0.05^{def}	5.99 ±0.05^{c}	4.25 ±0.25^{d}	21.77±0.25^{c}
S6-TC12	4.85 ±0.02^{ab}	7.21 ±0.05^{c}	6.27 ±0.02^{b}	4.53 ±0.02^{bc}	22.87±0.06^{b}
S6-TC16	4.99 ±0.04^{a}	7.85 ±0.07^{a}	6.60 ±0.05^{a}	4.83 ±0.06^{a}	24.27±0.21^{a}

[1)] N-0=gelatinized native high-amylose corn starch; N-I/TC4-16=native high-amylose corn starches stored in isothermal condition (I) at 4°C and temperature-cycling condition (TC) of 4°C and 70°C for 4-16 days at 4 days interval; S6-0=gelatinized starch after 60 min sonication; S6-I/TC4-16=60 min sonicated starches stored in isothermal condition (I) at 4°C and temperature-cycling condition (TC) of 4°C and 70°C for 4-16 days at 4 days interval.

[2)] The values with different superscripts in the same column are significantly different (p<0.05) by Tukey's honest significant difference (HSD) test.

4. Solid-state ^{13}C cross-polarization and magic-angle spinning (CP/MAS) nuclear magnetic resonance (NMR) spectra

In ^{13}C CP/MAS NMR spectra of all retrograded samples, the intensities of starch samples rose as the storage time increased (Figure 9). S6 retrograded samples and TC groups showed higher intensities compared with retrograded native HACS samples and isothermal storage groups, respectively.

In retrograded starches, the proportion of ordered structure, indicating double-helical content, increased gradually with the storage period (Table 13). This increasing tendency was also observed in peak intensity. It corresponded to the results of thermal transition properties and relative crystallinity (Table 9, 10, and 12). The proportion of double-helical structure acquired by ^{13}C CP/MAS NMR was higher than relative crystallinity obtained by XRD, because XRD method does not detect the irregularly packed structures (Gidley & Bociek, 1985). In the retrograded samples, an increase in the relative crystallinity of XRD was higher than that in the double-helical structure of ^{13}C CP/MAS NMR, suggesting that irregularly arrayed crystallites could build the ordered crystalline structure during retrogradation.

The ratio of ordered structure to amorphous structure (O/A ratio) of S6-0 was 0.29, which was lower than that of N-0 (0.31), but the increase in the

ratio by retrogradation in S6 samples was twice as high as that of native HACS. Specifically, the extent of increase in the O/A ratio of S6 samples during retrogradation was 0.24, which was the difference between S6-0 and S6-TC16. On the other hand, the O/A ratio of native HACS increased by 0.12 during retrogradation, the difference between N-0 and N-TC16. It indicated that reduced double helix content in S6 by sonication increased again during retrogradation. Furthermore, retrograded S6 samples had more double-helical structure than retrograded native HACS did, because the decreases in the molecular weight of AM and AP by sonication caused a high extent of retrogradation.

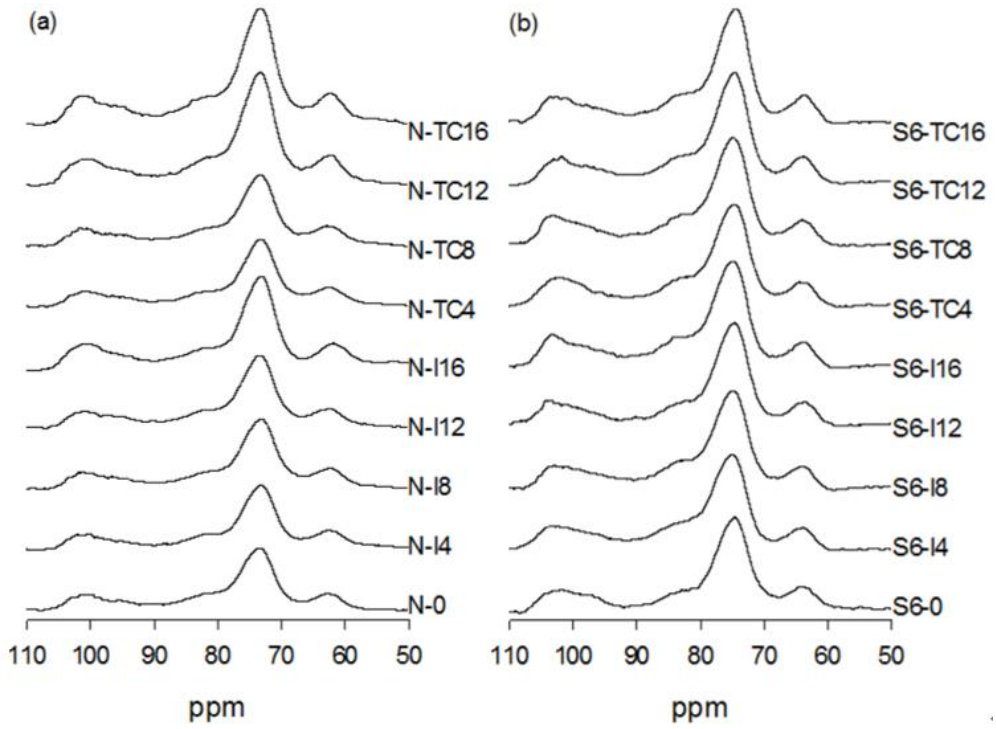

Figure 9. ^{13}C CP/MAS NMR spectra of (a) retrograded HACS=retrograded high-amylose corn starch and (b) retrograded S6=retrograded 60 min sonicated starch.

Table 13. The proportions of ordered structures of retrograded starches

Sample[1)]	Ordered (%)[2)]	Amorphous (%)[3)]	O/A ratio[4)]
N-0	23.71	76.30	0.31
N-I4	26.57	73.44	0.36
N-I8	27.42	72.59	0.38
N-I12	27.56	72.44	0.38
N-I16	28.18	71.82	0.39
N-TC4	27.00	73.00	0.37
N-TC8	27.64	72.36	0.38
N-TC12	29.80	70.20	0.42
N-TC16	29.94	70.06	0.43
S6-0	22.77	77.23	0.29
S6-I4	28.81	71.19	0.40
S6-I8	30.95	69.05	0.45
S6-I12	31.75	68.25	0.47
S6-I16	33.00	67.01	0.49
S6-TC4	31.15	68.85	0.45
S6-TC8	33.04	66.96	0.49
S6-TC12	34.10	65.90	0.52
S6-TC16	34.70	65.30	0.53

[1)] N-0=gelatinized native high-amylose corn starch; N-I/TC4-16=native high-amylose corn starches stored in isothermal condition (I) at 4°C and temperature-cycling condition (TC) of 4°C and 70°C for 4-16 days at 4 days interval; S6-0=gelatinized starch after 60 min sonication; S6-I/TC4-16=60 min sonicated starches stored in isothermal condition (I) at 4°C and temperature-cycling condition (TC) of 4°C and 70°C for 4-16 days at 4 days interval.

[2)] The proportion of ordered structure.

[3)] The proportion of amorphous structure.

[4)] The ratio of ordered structure to amorphous structure.

5. Resistant starch (RS) content

Resistant starch contents of all the retrograded starches are shown in Table 14. S6-0 showed a lower RS content than N-0, but sonication treatment accelerated the retrogradation in the retrograded S6 samples, and a higher RS content was observed compared with the retrograded native HACS samples. TC samples had higher RS contents than isothermal samples in the same storage period, and RS contents increased with the storage time. However, there was no significant difference (p>0.05) between the 12 days and 16 days retrograded samples in both native HACS and S6 samples due to the deceleration of retrogradation, which was supported by the results of corresponding parameters in DSC, XRD and NMR.

HACS is comprised primarily of numerous α-1,4 glycosidic linkages and forms linear configuration, which made the enzyme inaccessible to starch and constitutes the RS2. In addition, inherent amylose-lipid complex of HACS induces the formation of RS5. N-0 and S6-0 not to be influenced by the retrogradation, and therefore, RS in these samples was mainly composed of RS2 and RS5. An increase in RS3 with the extended retrogradation period contributed to the increment of RS content in retrograded samples.

Several starches including waxy potato starch, normal corn and waxy corn starches, treated under the TC retrogradation, showed less than 30% RS

contents based on the method of Englyst et al. (Tian et al., 2012; Xie et al., 2014; Zhang et al., 2011; Zhou & Lim, 2012). However, RS measured by the Englyst assay is not truly resistant to digestion, and there was inconsistency of RS content assayed by the Englyst method and AOAC/AACC method (Zhang et al., 2006). On the other hand, Zhou (2013) analyzed the RS in retrograded waxy and normal corn starches using both assays. After the storage at 4°C for 8 days, waxy and normal corn starches revealed 5.9% and 9.6% lower RS content, respectively, in the AOAC/AACC assay compared with the Englyst method. N-I8 (24.63%) and S6-I8 (33.47%) in the current study had identical condition of 8 days storage at 4°C and showed higher RS contents than waxy and normal corn starches.

Compared with the HACS, which revealed apparent AM content of 50.80%, those samples used in previous studies contained less than 20% AM contents (Zhou et al., 2013; Zhou & Lim, 2012). This difference in AM content made the rate of nucleation high in HACS, which was the most important factor to overcome the rate-limiting-step of retrogradation. Furthermore, the sonication pretreatment before retrogradation, performed only in this study, induced a decrease in molecular weight of starch. Numerous AM nuclei and dense arrangement of AP contributed to the acceleration of retrogradation. Thus, RS content obtained from this study was higher than those in other studies (Zhang et al., 2006; Zhou et al., 2013).

Table 14. Resistant starch (RS) contents of retrograded starches

Sample[1)]	Resistant starch content (%)
N-0	15.80±0.26^{i}[2)]
N-I4	21.96±0.64^{h}
N-I8	24.63±0.77^{fg}
N-I12	25.38±1.03^{fg}
N-I16	25.96±0.75^{f}
N-TC4	22.80±0.68^{gh}
N-TC8	25.40±0.49^{f}
N-TC12	29.11±0.81^{e}
N-TC16	30.63±1.07^{e}
S6-0	15.05±0.61^{i}
S6-I4	28.93±0.79^{e}
S6-I8	33.47±1.35^{d}
S6-I12	36.07±1.00^{bc}
S6-I16	37.91±0.76^{b}
S6-TC4	33.68±1.13^{cd}
S6-TC8	38.27±1.10^{b}
S6-TC12	41.28±0.35^{a}
S6-TC16	42.69±0.80^{a}

[1)] N-0=gelatinized native high-amylose corn starch; N-I/TC4-16=native high-amylose corn starches stored in isothermal condition (I) at 4°C and temperature-cycling condition (TC) of 4°C and 70°C for 4-16 days at 4 days interval; S6-0=gelatinized starch after 60 min sonication; S6-I/TC4-16=60 min sonicated starches stored in isothermal condition (I) at 4°C and temperature-cycling condition (TC) of 4°C and 70°C for 4-16 days at 4 days interval.

[2)] The values with different superscripts in the same column are significantly different (p<0.05) by Tukey's honest significant difference (HSD) test.

6. Principal component analysis of structural and retrogradation properties in relation to sonication and retrogradation

Principal component analysis (PCA) was conducted to summarize the results from structural and retrogradation properties induced by sonication and retrogradation (Figure 10). PCA loading plots provided an overview of the similarities and differences among samples treated with sonication and retrogradation conditions based on the relationships underlying the measured structural and retrogradation characteristics. The first and second principal components (PCs) could explain 54.05% and 29.25% of total variance, respectively, indicating that the first two PCs explained most of the variability underlying the experimental data. PC1 majorly separated the samples and properties in relation to the presence or absence of sonication while PC2 separated those by retrogradation period and the properties differentiated by the storage period.

High positive correlation was indicated among peak intensity (13°, 17.2°, 20°, and 23°), relative crystallinity, O/A ratio, proportion of ordered structure, thermal properties (T_{o1}, T_{p1}, T_{c1}, T_{o3}, T_{p3}, $\Sigma(\Delta H)$, $\Delta H1$, and $\Delta H3$) and RS loaded positively on PC1. Samples N-TC12, N-TC16, and retrograded S6, except S-I4, were loaded close to these properties indicating that these

attributes were strong in starches with high degree of retrogradation derived by sonication. Samples, S-I4 and retrograded native HACS, except N-TC12 and N-TC16, were located close each other along with T_{c3} and proportion of amorphous structure indicating that these attributes were strong in starches with relatively lower degree of retrogradation. N-0 and S6-0 were also located closely on PC1 in the negative direction, indicating that amorphous structure was strong in gelatinized starches.

Meanwhile, S6-I4 and S6-TC4 were loaded oppositely from PC1, and native HACS samples, retrograded more than 12 days under the different conditions of temperature, were also loaded oppositely from PC1. It may be explained by the effect of TC retrogradation.

All retrograded native HACS starches and sonicated starches retrograded less than 8 days were located positively on PC2 along with high relative crystallinity and peak intensity (13°, 17.2°, 20°, and 23°), relative crystallinity, O/A ratio, proportion of ordered structure, thermal properties (T_{o1}, T_{p1}, T_{c1}, $\Sigma(\Delta H)$ $\Delta H1$, and $\Delta H3$), and RS revealing these properties were induced by high retrogradation. T_{o3}, T_{p3}, T_{c3} and proportion of amorphous structure were highly loaded on PC2 in the negative direction where N-0, S6-0, S6-I12, S6-I16, S6-TC12, and S6-TC16 were located, demonstrating that parameters of DSC peak III were strong in sonicated starches retrograded more than 12 days. Gradual decreases in T_{p3} and T_{c3}, which resulted from the

extended retrogradation of AM and formation of perfect crystallites, caused its negative loading on PC2.

In summary, PCA loading plot clearly manifested and summarized the effects of sonication, longer period storage, and TC retrogradation. Starch structure became more ordered due to the retrogradation, and the results of transition enthalpies and relative crystallinity revealed that perfect crystallites were generated. These alterations in starch gradually increased the RS content during retrogradation.

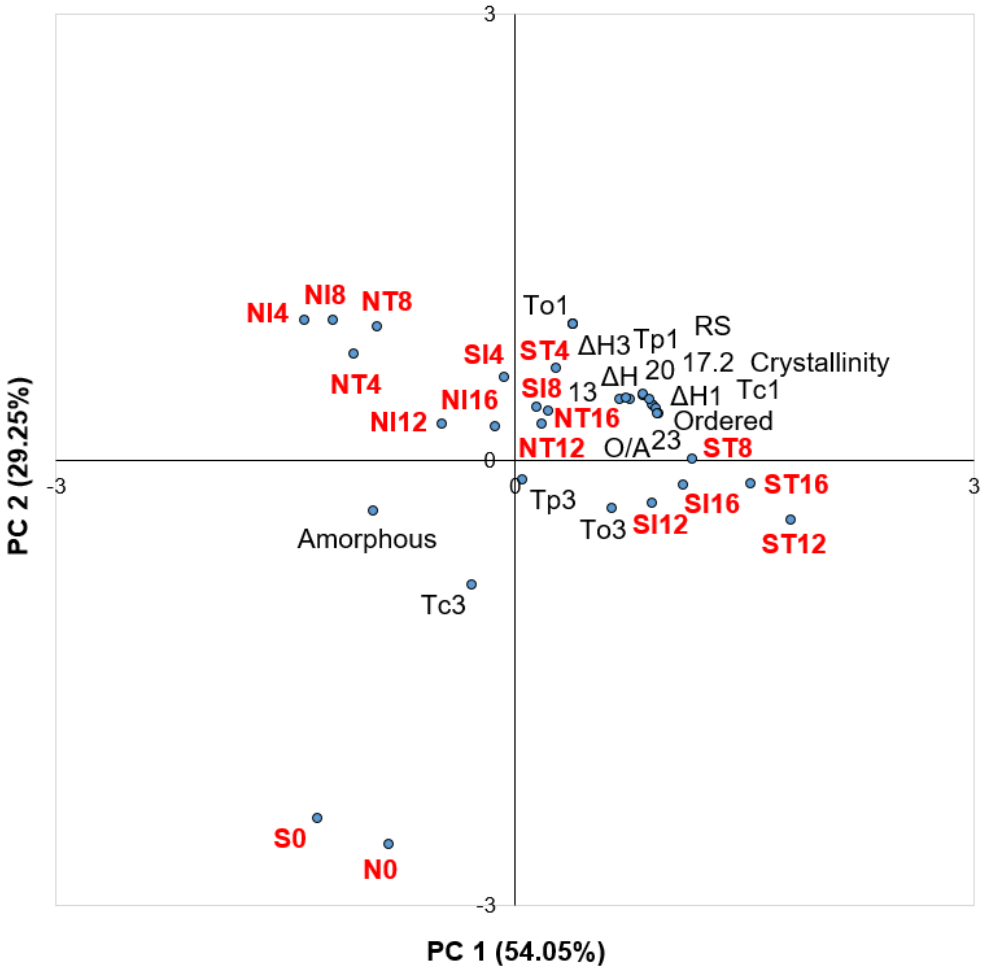

Figure 10. Principal component analysis: loading plot of PC1 and PC2 describing the variation among properties of retrograded starch.

13: peak intensity of 13°; 17.2: peak intensity of 17.2°; 20: peak intensity of 20°; 23: peak intensity of 23°; Amorphous: proportion of amorphous structure; Crystallinity: relative crystallinity; O/A: ratio of ordered structure to amorphous structure; Ordered: proportion of ordered structure; RS: resistant starch content; T_{c1}: conclusion temperature in peak I; T_{o1}: onset temperature in peak I; T_{p1}: peak temperature in peak I; $\Delta H1$: enthalpy change of melting in peak I; T_{c3}: conclusion temperature in peak III; T_{o3}: onset temperature in peak III; T_{p3}: peak temperature in peak III; $\Delta H3$: enthalpy change of melting in peak III; ΔH: sum of

melting enthalpies; N-0=gelatinized native high-amylose corn starch; N-I/TC4-16=native high-amylose corn starches stored in isothermal condition (I) at 4°C and temperature-cycling condition (TC) of 4°C and 70°C for 4-16 days at 4 days interval; S6-0=gelatinized starch after 60 min sonication; S6-I/TC4-16=60 min sonicated starches stored in isothermal condition (I) at 4°C and temperature-cycling condition (TC) of 4°C and 70°C for 4-16 days at 4 days interval.

CONCLUSIONS

The effects of structural properties of sonicated starch on the retrogradation were investigated in the current study. Also, this study showed the effects of TC retrogradation on the structural and retrogradation characteristics and resistant starch content.

In regards to the several structural properties, the alterations of AM and AP by sonication were explained respectively and applied to TC retrogradation. AM single helices and random coils were disrupted by sonication, followed by fast transition of shortened coils to single helix and formation of AM double helices. This phenomenon contributes to the acceleration and overcoming of nucleation stage of TC retrogradation, with numerous AM double helices broken by sonication. Also, disintegration of cluster in AP by hydrolysis of amorphous region made dense arrangement of AP in propagation step of retrogradation. Thus, degree of retrogradation, including RS content, was higher in retrograded S6 samples than retrograded HACS because of accelerated nucleation and propagation. Furthermore, compared with isothermal storage, temperature-cycling of stepwise nucleation and propagation caused a higher extent of retrogradation at the same period. Longer period of retrogradation also resulted in the formation of perfect crystallites and more double helices due to the repeated nucleation and

propagation step.

Overall experimental data in the present study showed that sonication treatment induced appropriate structural properties for the retrogradation. Also, there were more changes in retrogradation and structural characteristics and RS contents under the temperature-cycling conditions compared with isothermal storage. This study contributes to deeper assessment of the structural alteration in starch by sonication, and gives basic understanding for the retrogradation of sonicated starch. Moreover, these findings suggest alternative applications of the sonicated starch as healthy-functional ingredient containing high RS, and utilization of sonication is extended to health industry beyond food processing and preservation. Optimization of sonication treatment condition for retrogradation, including frequency, power and amplitude, is required to study. Also, dual modification of sonication and retrogradation would be applied to other starches from different botanical sources containing various ratio of AM and AP.

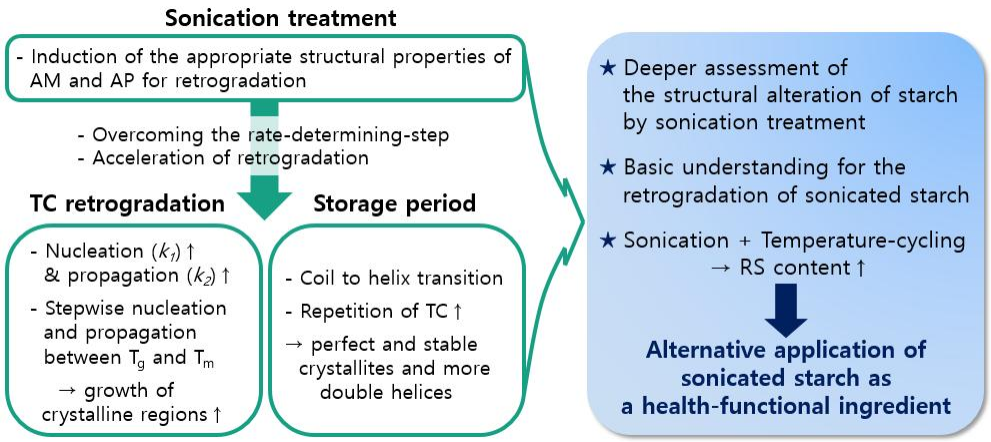

REFERENCES

AACC. (2000). *Approved Methods of the AACC International, Method 61-03* (10th ed.). St. Paul: AACC International.

AACC. (2002). *Approved Methods of the AACC International, Method 32-40.01* (11th ed.). St.Paul: AACC International Publisher.

Ambigaipalan, P., Hoover, R., Donner, E., & Liu, Q. (2013). Retrogradation characteristics of pulse starches. *Food Research International, 54*, 203-212.

Arık Kibar, E. A., Gönenç, İ., & Us, F. (2011). Modeling of retrogradation of waxy and normal corn starches. *International Journal of Food Properties, 14*, 954-967.

Arnold, G., Leiteritz, L., Zahn, S., & Rohm, H. (2009). Ultrasonic cutting of cheese: Composition affects cutting work reduction and energy demand. *International Dairy Journal, 19*, 314-320.

Atichokudomchai, N., Varavinit, S., & Chinachoti, P. (2004). A study of ordered structure in acid-modified tapioca starch by 13C CP/MAS solid-state NMR. *Carbohydrate Polymers, 58*, 383-389.

Ba, K., Aguedo, M., Tine, E., Paquot, M., Destain, J., & Thonart, P. (2013). Hydrolysis of starches and flours by sorghum malt amylases for dextrins production. *European Food Research and Technology, 236*, 905-918.

Baik, M. Y., Kim, K. J., Cheon, K. C., Ha, Y. C., & Kim, W. S. (1997). Recrystallization kinetics and glass transition of rice starch gel system. *Journal of Agricultural and Food Chemistry, 45*, 4242-4248.

Barichello, V., Yada, R. Y., Coffin, R. H., & Stanley, D. W. (1990). Low temperature sweetening in susceptible and resistant potatoes: starch structure and composition. *Journal of Food Science, 55*, 1054-1059.

Bartsch, M., & Schmidt-Naake, G. (2006). Application of nitroxide-terminated polymers prepared by sonochemical degradation in the synthesis of block copolymers. *Macromolecular Chemistry and*

Physics, 207, 209-215.

Biliaderis, C. G., Maurice, T. J., & Vose, J. R. (1980). Starch gelatinization phenomena studied by differential scanning calorimetry. *Journal of Food Science, 45*, 1669-1674.

Birt, D. F., Boylston, T., Hendrich, S., Jane, J. L., Hollis, J., Li, L., McClelland, J., Moore, S., Phillips, G. J., Rowling, M., Schalinske, K., Scott, M. P., & Whitley, E. M. (2013). Resistant starch: promise for improving human health. *Advances in Nutrition, 4*, 587-601.

Bradbury, A. G. W., & Bello, A. B. (1993). Determination of molecular size distribution of starch and debranched starch by a single procedure using high-performance size-exclusion chromatography. *Cereal Chemisty, 70*, 543-547.

Brouns, F., Kettlitz, B., & Arrigoni, E. (2002). Resistant starch and "the butyrate revolution". *Trends in Food Science & Technology, 13*, 251-261.

Brown, I. L., McNaught, K. J., & Moloney, E. (1995). Hi-maize: new directions in starch technology and nutrition. *Food Australia, 47*, 272-275.

Chan, H.-T., Bhat, R., & Karim, A. A. (2010). Effects of sodium dodecyl sulphate and sonication treatment on physicochemical properties of starch. *Food Chemistry, 120*, 703-709.

Chang, S., & Liu, L. (1991). Retrogradation of rice starches studied by differential scanning calorimetry and influence of sugars, NaCl and lipids. *Journal of Food Science, 56*, 564-566.

Chang, Y. H., & Lin, J. H. (2007). Effects of molecular size and structure of amylopectin on the retrogradation thermal properties of waxy rice and waxy cornstarches. *Food Hydrocolloids, 21*, 645-653.

Cheetham, N. W. H., & Tao, L. (1998). Variation in crystalline type with amylose content in maize starch granules : an X-ray powder diffraction study. *Carbohydrate Polymers, 36*, 277-284.

Chemat, F., Zill e, H., & Khan, M. K. (2011). Applications of ultrasound in food technology: Processing, preservation and extraction. *Ultrasonics*

Sonochemisty, 18, 813-835.

Chung, H. J., Jeong, H. Y., & Lim, S. T. (2003). Effects of acid hydrolysis and defatting on crystallinity and pasting properties of freeze-thawed high amylose corn starch. *Carbohydrate Polymers, 54*, 449-455.

Conde-Petit, B., Nuessli, J., Handschin, S., & Escher, F. (1998). Comparative characterisation of aqueous starch dispersions by light microscopy, rheometry and iodine binding behaviour. *Starch - Stärke, 50*, 184-192.

Czechowska-Biskup, R., Rokita, B., Lotfy, S., Ulanski, P., & Rosiak, J. M. (2005). Degradation of chitosan and starch by 360-kHz ultrasound. *Carbohydrate Polymers, 60*, 175-184.

Czuchajowska, Z., Klamczynski, A., Paszczynska, B., & Baik, B. K. (1998). Structure and functionality of barley starches. *Cereal Chemistry, 75*, 747-754.

Durrani, C. M., & Donald, A. M. (1995). Physical Characterisation of Amylopectin Gels. *Polymer Gels and Networks, 3*, 1-27.

Eerlingen, R. C., Crombez, M., & Delcour, J. A. (1993). Enzyme-resistant starch. I. Quantitative and qualitative influence of incubation time and temperature of autoclaved starch on resistant starch formation. *Cereal Chemisty, 70*, 339-344.

Eliasson, A.-C., & Gudmundsson, M. (2006). Starch: Physicochemical and functional aspects. In Eliasson. A.-C. (Ed.), *Carbohydrates in Food* 2nd ed., Boca Raton: CRC/Taylor & Francis, pp 391-469.

Englyst, H., Wiggins, H. S., & Cummings, J. H. (1982). Determination of the non-starch polysaccharides in plant foods by gas-liquid chromatography of constituent sugars as alditol acetates. *Analyst, 107*, 307-318.

Englyst, H. N., Kingman, S. M., & Cummings, J. H. (1992). Classification and measurement of nutritionally important starch fractions. *European Journal of Clinical Nutrition, 46*, S33-50.

Fan, J., & Marks, B. P. (1998). Retrogradation kinetics of rice flours as influenced by cultivar. *Cereal Chemisty, 75*, 153-155.

Fearn, T., & Russell, P. L. (1982). A kinetic study of bread staling by differential scanning calorimetry. The effect of loaf specific volume. *Journal of the Science of Food and Agriculture, 33*, 537-548.

Fredriksson, H., Silverio, J., Andersson, R., Eliasson, A.-C., & Åman, P. (1998). The influence of amylose and amylopectin characteristics on gelatinization and retrogradation properties of different starches. *Carbohydrate Polymers, 35*, 119-134.

Fuentes-Zaragoza, E., Sánchez-Zapata, E., Sendra, E., Sayas, E., Navarro, C., Fernández-López, J., & Pérez-Alvarez, J. A. (2011). Resistant starch as prebiotic: A review. *Starch - Stärke, 63*, 406-415.

Genkina, N. K., Wikman, J., Bertoft, E., & Yuryev, V. P. (2007). Effects of structural imperfection on gelatinization chracteristics of amylopectin starches with A- and B-Type crystallinity. *Biomacromolecules, 8*, 2329-2335.

Gidley, M. J. (1985). Quantification of the structural features of starch polysaccharides by N.M.R. spectroscopy. *Carbohydrate Research, 139*, 85-93.

Gidley, M. J., & Bociek, S. M. (1985). Molecular organization in starches: a carbon 13 CP/MAS NMR study. *Journal of the American Chemical Society, 107*, 7040-7044.

Gidley, M. J., & Bociek, S. M. (1988). 13C CP/MAS NMR studies of amylose inclusion complexes, cyclodextrins, and the amorphous phase of starch granules: relationships between glycosidic linkage conformaton and solid-state 13C chemical shifts. *Journal of the American Chemical Society, 110*, 3820-3829.

Gidley, M. J., & Bulpin, P. V. (1989). Aggregation of amylose in aqueous systems: the effect of chain length on phase behavior and aggregation kinetics. *Macromolecules, 22*, 341-346.

Gidley, M. J., Cooke, D., Darke, A. H., Hoffmann, R. A., Russell, A. L., & Greenwell, P. (1995). Molecular order and structure in enzyme-resistant retrograded starch. *Carbohydrate Polymers, 28*, 23-31.

Granfeldt, Y., Drews, A., & Bjorck, I. (1995). Arepas made from high amylose corn flour produce favorably low glucose and insulin

responses in healthy humans. *The Journal of Nutrition, 125*, 459.

Harder, H., Khol-Parisini, A., & Zebeli, Q. (2015). Treatments with organic acids and pullulanase differently affect resistant starch and fiber composition in flour of various barley genotypes (*Hordeum vulgare L.*). *Starch - Stärke, 67*, 512-520.

Hasjim, J., Lee, S. O., Hendrich, S., Setiawan, S., Ai, Y., & Jane, J. L. (2010). Characterization of a novel resistant-starch and its effects on postprandial plasma-glucose and insulin responses. *Cereal Chemistry, 87*, 257-262.

Heineck, M. E., Cardoso, M. B., Giacomelli, F. C., & da Silveira, N. P. (2008). Evidences of amylose coil-to-helix transition in stored dilute solutions. *Polymer, 49*, 4386-4392.

Higgins, J. A. (2004). Resistant starch: metabolic effects and potential health benefits. *Journal of AOAC International, 87*, 761-768.

Hoover, R. (2000). Acid-treated starches. *Food Reviews International, 16*, 369-392.

Hoover, R., & Vasanthan, T. (1994). Effect of heat-moisture treatment on the structure and physicochemical properties of cereal, legume, and tuber starches. *Carbohydrate Research, 252*, 33-53.

Hu, A., Lu, J., Zheng, J., Sun, J., Yang, L., Zhang, X., Zhang, Y., & Lin, Q. (2013). Ultrasonically aided enzymatical effects on the properties and structure of mung bean starch. *Innovative Food Science and Emerging Technologies, 20*, 146-151.

Inaba, H., Hatanaka, Y., Adachi, T., Matsumura, Y., & Mori, T. (1994). Changes with retrogradation of mechanical and textural properties of gels from various starches. *Carbohydrate Polymers, 24*, 31-40.

Isono, Y., Kumagai, T., & Watanabe, T. (1994). Ultrasonic degradation of waxy rice starch. *Bioscience, Biotechnology, and Biochemistry, 58*, 1799-1802.

Jankowski, T., & Rha, C. K. (1986). Retrogradation of starch in cooked wheat. *Starch - Stärke, 38*, 6-9.

Jiranuntakul, W., Puttanlek, C., Rungsardthong, V., Puncha-arnon, S., & Uttapap, D. (2011). Microstructural and physicochemical properties of heat-moisture treated waxy and normal starches. *Journal of Food Engineering, 104*, 246-258.

Johnston, K. L., Thomas, E. L., Bell, J. D., Frost, G. S., & Robertson, M. D. (2010). Resistant starch improves insulin sensitivity in metabolic syndrome. *Diabetic Medicine, 27*, 391-397.

Kaletunç, G., & Breslauer, K. (2003). *Characterization of cereals and flours : properties, analysis, and applications*. New York: Marcel Dekker, pp 65-116.

Kang, N., Zuo, Y. J., Hilliou, L., Ashokkumar, M., & Hemar, Y. (2016). Viscosity and hydrodynamic radius relationship of high-power ultrasound depolymerised starch pastes with different amylose content. *Food Hydrocolloids, 52*, 183-191.

Kardos, N., & Luche, J. L. (2001). Sonochemistry of carbohydrate compounds. *Carbohydrate Research, 332*, 115-131.

Karim, A. A., Norziah, M. H., & Seow, C. C. (2000). Methods for the study of starch retrogradation. *Food Chemistry, 71*, 9-36.

Kim, W. K., Chung, M. K., Kang, N. E., Kim, M. H., & Park, O. J. (2003). Effect of resistant starch from corn or rice on glucose control, colonic events, and blood lipid concentrations in streptozotocin-induced diabetic rats. *The Journal of Nutritional Biochemistry, 14*, 166-172.

Kitamura, S., Hakozaki, K., & Kuge, T. (1994). Effects of molecular weight on the retrogradation of amylose. In K. Nishinari & E. Doi (Eds.), *Food Hydrocolloids*, New York: Springer US, pp 179-182.

Kulp, K., & Ponte, J. G. (2000). *Handbook of cereal science and technology* (2nd ed., rev. and expanded.. ed.). New York: Marcel Dekker, pp 31-80.

Kyllönen, H. M., Pirkonen, P., & Nyström, M. (2005). Membrane filtration enhanced by ultrasound: a review. *Desalination, 181*, 319-335.

Leong, Y. H., Karim, A. A., & Norziah, M. H. (2007). Effect of pullulanase debranching of sago (*Metroxylon sagu*) starch at subgelatinization temperature on the yield of resistant starch. *Starch - Stärke, 59*, 21-32.

Levenspiel, O. (1999). *Chemical reaction engineering* (3rd ed.). New York: Wiley, pp 170-206.

Lin, P. Y., & Czuchajowska, Z. (1997). Starch properties and stability of club and soft white winter wheats from the Pacific Northwest of the United States. *Cereal Chemistry, 74*, 639-646.

Lopez-Rubio, A., Flanagan, B. M., Gilbert, E. P., & Gidley, M. J. (2008). A novel approach for calculating starch crystallinity and its correlation with double helix content: a combined XRD and NMR study. *Biopolymers, 89*, 761-768.

Luo, Z., Fu, X., He, X., Luo, F., Gao, Q., & Yu, S. (2008). Effect of ultrasonic treatment on the physicochemical properties of maize starches differing in amylose content. *Starch - Stärke, 60*, 646-653.

Maki, K. C., Pelkman, C. L., Finocchiaro, E. T., Kelley, K. M., Lawless, A. L., Schild, A. L., & Rains, T. M. (2012). Resistant starch from high-amylose maize increases insulin sensitivity in overweight and obese men. *The Journal of Nutrition, 142*, 717-723.

Mali, S., Karam, L. B., Ramos, L. P., & Grossmann, M. V. E. (2004). Relationships among the composition and physicochemical properties of starches with the characteristics of their films. *Journal of Agricultural and Food Chemistry, 52*, 7720-7725.

Mañas, P., Pagán, R., Raso, J., Sala, F. J., & Condón, S. (2000). Inactivation of Salmonella Enteritidis, Salmonella Typhimurium, and Salmonella Senftenberg by ultrasonic waves under pressure. *Journal of Food Protection, 63*, 451-456.

Manners, D. J. (1989). Recent developments in our understanding of amylopectin structure. *Carbohydrate Polymers, 11*, 87-112.

McCleary, B. V., McNally, M., & Rossiter, P. (2002). Measurement of resistant starch by enzymatic digestion in starch and selected plant materials: collaborative study. *Journal of AOAC International, 85*, 1103-1111.

McIver, R. G., Axford, D. W. E., Colwell, K. H., & Elton, G. A. H. (1968). Kinetic study of the retrogradation of gelatinised starch. *Journal of the Science of Food and Agriculture, 19*, 560-563.

Miles, M. J., Morris, V. J., Orford, P. D., & Ring, S. G. (1985). The roles of amylose and amylopectin in the gelation and retrogradation of starch. *Carbohydrate Research, 135*, 271-281.

Murphy, M. M., Douglass, J. S., & Birkett, A. (2008). Resistant starch intakes in the United States. *Journal of the American Dietetic Association, 108*, 67-78.

Muthukumaran, S., Kentish, S., Ashokkumar, M., & Stevens, G. (2005). Mechanisms for the ultrasonic enhancement of dairy whey ultrafiltration. *Journal of Membrane Science, 258*, 106-114.

Nara, S., & Komiya, T. (1983). Studies on the relationship between water-satured state and crystallinity by the diffraction method for moistened potato starch. *Starch - Stärke, 35*, 407-410.

Nitsch, E. (1995). Process for the production of starch degradation products with a narrow molecular weight distribution. U.S. patent 5424302.

Nugent, A. P. (2005). Health properties of resistant starch. *Nutrition Bulletin, 30*, 27-54.

Ottenhof, M. A., & Farhat, I. A. (2004). Starch retrogradation. *Biotechnology and Genetic Engineering Reviews, 21*, 215-228.

Park, E. Y., Baik, B. K., & Lim, S. T. (2009). Influences of temperature-cycled storage on retrogradation and in vitro digestibility of waxy maize starch gel. *Journal of Cereal Science, 50*, 43-48.

Peres, G. L., Leite, D. C., & Silveira, N. P. D. (2015). Ultrasound effect on molecular weight reduction of amylopectin. *Starch - Stärke, 67*, 407-414.

Pineda-Gómez, P., Angel-Gil, N. C., Valencia-Muñoz, C., Rosales-Rivera, A., & Rodríguez-García, M. E. (2014). Thermal degradation of starch sources: green banana, potato, cassava, and corn - kinetic study by non-isothermal procedures. *Starch - Stärke, 66*, 691-699.

Poinot, T., Benyahia, K., Govin, A., Jeanmaire, T., & Grosseau, P. (2013). Use of ultrasonic degradation to study the molecular weight influence of polymeric admixtures for mortars. *Construction and Building Materials, 47*, 1046-1052.

Riera, E., Gallego-Juarez, J. A., & Mason, T. J. (2006). Airborne ultrasound for the precipitation of smokes and powders and the destruction of foams. *Ultrasonics Sonochemistry, 13*, 107-116.

Sajilata, M. G., Singhal, R. S., & Kulkarni, P. R. (2006). Resistant starch-a review. *Comprehensive Reviews in Food Science and Food Safety, 5*, 1-17.

Schneider, Y., Zahn, S., & Rohm, H. (2008). Power requirements of the high-frequency generator in ultrasonic cutting of foods. *Journal of Food Engineering, 86*, 61-67.

Sharma, A., Yadav, B. S., & Ritika, B. Y. (2008). Resistant starch: physiological roles and food applications. *Food Reviews International, 24*, 193-234.

Silverio, J., Fredriksson, H., Andersson, R., Eliasson, A.-C., & Åman, P. (2000). The effect of temperature cycling on the amylopectin retrogradation of starches with different amylopectin unit-chain length distribution. *Carbohydrate Polymers, 42*, 175-184.

Skrabanja, V., Liljeberg Elmstahl, H. G., Kreft, I., & Bjorck, I. M. (2001). Nutritional properties of starch in buckwheat products: studies in vitro and in vivo. *Journal of Agricultural and Food Chemistry, 49*, 490-496.

Sujka, M., & Jamroz, J. (2013). Ultrasound-treated starch: SEM and TEM imaging, and functional behaviour. *Food Hydrocolloids, 31*, 413-419.

Tanaka, T., Tsutsui, A., Gotanda, R., Sasayama, S., Yamamoto, K., & Kadokawa, J. (2015). Synthesis of amylose-polyether inclusion supremolecular polymers by vine-twining polymerization using maltoheptaose-functionailized poly(tetradhydrofuran) as a primer-guest conjugate. *Journal of Applied Glycoscience, 62*, 135-141.

Tian, Y., Zhang, L., Xu, X., Xie, Z., Zhao, J., & Jin, Z. (2012). Effect of temperature-cycled retrogradation on slow digestibility of waxy rice starch. *Internation Journal of Biological Macromolecules, 51*, 1024-1027.

Tian, Y., Zhu, Y., Bashari, M., Hu, X., Xu, X., & Jin, Z. (2013). Identification and releasing characteristics of high-amylose corn starch-cinnamaldehyde inclusion complex prepared using ultrasound

treatment. *Carbohydrate Polymers, 91*, 586-589.

Van Soest, J. J. G., De Wit, D., Tournois, H., & Vliegenthart, J. F. G. (1994). Retrogradation of potato starch as studied by fourier transform infrared spectroscopy. *Starch - Stärke, 46*, 453-457.

Voet, D., Voet, J. G. P., Charlotte, W., Judith, G. V., & Charlotte, W. P. (2013). *Fundamentals of biochemistry: life at the molecular level*. New York: Wiley, pp 517-550.

Wang, S., Li, C., Copeland, L., Niu, Q., & Wang, S. (2015). Starch retrogradation: a comprehensive review. *Comprehensive Reviews in Food Science and Food Safety, 14*, 568-585.

Ward, K. E. J., Hoseney, R. C., & Seib, P. A. (1994). Retrogradations of amylopectin from maize and wheat starches. *Cereal Chemistry, 71*, 150-155.

Whistler, R. L., Bemiller, J. N., & Paschell, E. F. (1984). Organization of starch granules. In D. French (Ed.), *Starch: Chemistry and Technology*, New York: Academic Press, pp 183-247.

Xie, Y. Y., Hu, X. P., Jin, Z. Y., Xu, X. M., & Chen, H. Q. (2014). Effect of temperature-cycled retrogradation on in vitro digestibility and structural characteristics of waxy potato starch. *International Journal of Biological Macromolecules, 67*, 79-84.

Xu, J., Zhao, W., Ning, Y., Jin, Z., Xu, B., & Xu, X. (2012). Comparative study of spring dextrin impact on amylose retrogradation. *Journal of Agricultural and Food Chemisty, 60*, 4970-4976.

Yao, Y., Zhang, J., & Ding, X. (2003). Partial β-amylolysis retards starch retrogradation in rice products. *Journal of Agricultural and Food Chemistry, 51*, 4066-4071.

Yuryev, V. P., Tomasik, P., & Bertoft, E. (2007). *Starch : achievements in understanding of structure and functionality*. New York: Nova Science Publishers, pp 49-64.

Zhang, B., Huang, Q., Luo, F., & Fu, X. (2012). Structural characterizations and digestibility of debranched high-amylose maize starch complexed with lauric acid. *Food Hydrocolloids, 28*, 174-181.

Zhang, G., Ao, Z., & Hamaker, B. R. (2006). Slow digestion property of native cereal starches. *Biomacromolecules, 7*, 3252-3258.

Zhang, H., Sun, B., Zhang, S., Zhu, Y., & Tian, Y. (2015). Inhibition of wheat starch retrogradation by tea derivatives. *Carbohydrate Polymers, 134*, 413-417.

Zhang, L., Hu, X., Xu, X., Jin, Z., & Tian, Y. (2011). Slowly digestible starch prepared from rice starches by temperature-cycled retrogradation. *Carbohydrate Polymers, 84*, 970-974.

Zhang, W., & Jackson, D. S. (1992). Retrogradation behavior of wheat starch gels with differing molecular profiles. *Journal of Food Science, 57, 1428-1432*.

Zheng, J., Li, Q., Hu, A., Yang, L., Lu, J., Zhang, X., & Lin, Q. (2013). Dual-frequency ultrasound effect on structure and properties of sweet potato starch. *Starch - Stärke, 65*, 621-627.

Zhou, X., Baik, B. K., Wang, R., & Lim, S. T. (2010). Retrogradation of waxy and normal corn starch gels by temperature cycling. *Journal of Cereal Science, 51*, 57-65.

Zhou, X., Chung, H. J., Kim, J. Y., & Lim, S. T. (2013). *In vitro* analyses of resistant starch in retrograded waxy and normal corn starches. *International Journal of Biological Macromolecules, 55*, 113-117.

Zhou, X., & Lim, S. T. (2012). Pasting viscosity and in vitro digestibility of retrograded waxy and normal corn starch powders. *Carbohydrate Polymers, 87*, 235-239.

Zhou, X., Wang, R., Yoo, S. H., & Lim, S. T. (2011). Water effect on the interaction between amylose and amylopectin during retrogradation. *Carbohydrate Polymers, 86*, 1671-1674.

Zhu, F. (2015). Impact of ultrasound on structure, physicochemical properties, modifications, and applications of starch. *Trends in Food Science & Technology, 43*, 1-17.

Zhu, J., Li, L., Chen, L., & Li, X. (2012). Study on supramolecular structural changes of ultrasonic treated potato starch granules. *Food Hydrocolloids, 29*, 116-122.

국문초록

이 연구에서는 고아밀로스 옥수수 녹말을 초음파 처리한 이후, 등온저장과 온도사이클링 조건으로 각각 16일간 노화 처리하였다. 초음파 처리에 의한 녹말의 분자량 감소로 말미암아 젤 여과 크로마토그래피의 아밀로펙틴과 아밀로스 피크 검출 시간이 모두 증가하였다. 수소-1 핵자기공명 분광법에서의 α-1,4 결합의 비율은 초음파 처리 시간이 증가함에 따라 조금씩 감소하였다. 아밀로스 이중 나선의 파괴는 아이오딘-녹말 복합체 형성에 필요한 공간을 생성하였으며, 이는 초음파 처리 녹말의 겉보기 아밀로스 함량의 증가를 일으켰다. 아밀로펙틴 결정은 초음파 처리로 점차적으로 붕괴하였고, 아밀로스 결정은 사라졌다. 고아밀로스 옥수수 녹말은 초음파 처리 하에 B형의 X-선 회절도형을 유지하였지만, 주요 피크의 강도와 상대적 결정화도는 감소하였다. 탄소-13 핵자기공명 분광법에서의 이중 나선 구조의 함량 또한 초음파 처리 시간의 연장에 따라 줄어들었다. 점차적인 평균 가지사슬 길이의 감소는 외측 사슬의 초음파에 대한 취약성을 나타내었다. 60분 초음파 처리한 시료가 구조적 특성의 차이가 가장 컸으며, 이 시료를 생녹말과 함

께 16일간 노화 처리하였다.

초음파 처리에 따라 대부분의 아밀로스 이중 나선이 파괴됨으로써 생성된 수많은 아밀로스 핵은 핵형성 단계를 촉진하였다. 무정형 영역에서의 α-1,4 결합의 가수분해로 아밀로스 랜덤 코일의 길이가 감소하여 단일 나선 구조로 빠르게 변화하였고 초음파에 의해 파괴된 아밀로스 단일 나선과 함께 아밀로스 이중 나선 형태의 핵을 형성하였다. 또한 무정형 영역의 분해로 아밀로펙틴 송이 구조가 분리되어 전파 단계에서 아밀로펙틴의 조밀한 배열을 유도하였다. 따라서, 전이 엔탈피, 주요 피크의 강도, 상대적 결정화도, 이중 나선 구조의 함량, 그리고 저항전분 함량이 60분 초음파 처리한 시료의 노화에서 더 높게 나타났다. 또한, 등온 저장과 비교하였을 때, 온도사이클링으로 인해 핵형성 단계와 전파 단계가 모두 가속화되었고, 노화 정도가 증가하였다. 아브라미 모델을 보완하는 비가역 연속 반응 모델로 분석한 결과, 핵형성과 전파 속도 역시 초음파 처리와 온도사이클링 처리한 그룹에서 더 높게 분석되었다. 그러므로, 초음파 처리한 녹말을 16일간 온도사이클링 노화한 시료가 가장 높은 노화 특성을 보유하였다.

초음파 처리는 노화에 적합한 구조적 특성을 유도하였고 또한

등온저장에 비해 온도사이클링 조건에서 구조적 특성, 노화 특성, 그리고 저항전분 함량이 더 크게 변화하였다. 요컨대 이 연구는 초음파 처리 녹말의 노화에 대한 연구를 새롭게 제시하였고, 온도사이클링 노화의 동역학적 모델을 확립하여 기초적 이해를 제공하였다. 이 연구에서 얻은 저항전분 함량이 증가된 초음파 처리 녹말은 식품산업에서 새로운 소재로서 활용될 수 있다.

주요어: 초음파, 고아밀로스 옥수수 녹말, 온도사이클링 노화, 아브라미 동역학 모델, 비가역 연속 반응 모델, 구조적 특성, 저항전분

학번: 2015-21802